

# Colour Decompositions of Multi-quark One-loop QCD Amplitudes

Harald Ita<sup>a,b,c</sup> and Kemal Ozeren<sup>a</sup>

<sup>a</sup>*Department of Physics and Astronomy, UCLA,  
Los Angeles, CA 90095-1547, USA*

<sup>b</sup>*Niels Bohr International Academy and Discovery Center, NBI,  
Blegdamsvej 17, DK-2100 Copenhagen, Denmark*

<sup>c</sup>*Raymond and Beverly Sackler School of Physics and Astronomy,  
Tel-Aviv University, Tel-Aviv 69978, Israel*

(Dated: November 18, 2011)

## Abstract

We describe the decomposition of one-loop QCD amplitudes in terms of colour-ordered building blocks. We give new expressions for the coefficients of QCD colour structures in terms of ordered objects called primitive amplitudes, for processes with up to seven partons. These results are needed in computations of high-multiplicity scattering cross sections in next-to-leading-order (NLO) QCD. We explain the origin of new relations between multi-quark primitive amplitudes which can be used to optimise efficiency of NLO computations. As a first application we compute the full-colour virtual contribution to the cross section for  $W + 4\text{-jet}$  production at the Large Hadron Collider, and verify that it is very well approximated by keeping only the leading terms in an expansion around the formal limit of a large number of colours.

PACS numbers: 11.15.Bt, 11.25.Db, 11.55.Bq, 12.38.-t, 12.38.Bx, 13.87.-a, 14.70.Fm

## I. INTRODUCTION

Scattering processes at the Large Hadron Collider (LHC) are dominated by the strong interactions. Of particular interest in the search for new physics are those which occur at high momentum transfer. These processes frequently mimic new physics signatures, and so a solid theoretical understanding is important to maximize the sensitivity of experimental searches. Perturbative calculations in QCD, including quantum corrections, provide first-principle predictions in this direction, strongly linking fundamental theory to experiment.

Recent years have seen remarkable progress in perturbative QCD, with new predictions at next-to-leading order (NLO) in the QCD coupling for many processes of interest at the LHC [1]. The present state-of-the-art studies of parton-level NLO QCD processes include three [2–6] or four [7–13] coloured final states. Such computations are challenging and rely on efficient algorithms for organising the various dynamic degrees of freedom, such as kinematics, spin and colour quantum numbers. In this article we focus on one particular aspect of these algorithms, namely the handling of the colour degrees of freedom for loop computations. Our results are of immediate use in modern approaches to NLO computations in QCD.

At tree level various approaches for dealing with colour have been developed with differing advantages. The colour-ordered approach groups together terms with identical  $SU(N_c)$  colour factors (where  $N_c$  is the number of colours). It was first developed for tree-level amplitudes in [14, 15] and later extended for use in loop computations in refs. [16–19]. This approach allows the symmetry properties and simplified kinematic dependence of ordered amplitudes to be exploited. Alternatively, one can treat colour simultaneously with the kinematic variables [20]. This colour-dressed method, most effectively implemented as a Berends-Giele recursion [21], has been shown to be very efficient for tree-level computation and is naturally applied to generic Standard Model processes [22–25].

At loop level the interaction of colour degrees of freedom is more complex, and requires refined techniques. For a large number of coloured final states the ordered approach has proved particularly useful (see e.g. [3–5, 11, 12]). For this colour organization an expansion in powers of  $1/N_c$  is naturally set up which allows for significant efficiency gains in the numerical phase space integration [5]; for a fixed integration error, fewer evaluations are needed for the smaller, but typically more time consuming, subleading-colour contributions [26].

The colour-ordered approach is also naturally suited to modern methods for loop computations using unitarity [17, 27, 28] and on-shell recursion [29–31]. In particular, generalised unitarity [19, 32, 33] and its numerical extension [31, 34–37] was first developed in the context of the colour-ordered approach. Ordered loop amplitudes have simplified analytic properties and can be built through unitarity cuts from ordered tree amplitudes. The division of the full amplitude into ordered pieces also leads to improved numerical control. By now a number of different methods for dealing with colour are in use for computing hard virtual scattering matrix elements [31, 38–43]. This includes colour sampling recursive approaches [10, 39], in analogy to those developed at tree level. More traditional methods to organise loop computations using colour information in the context of a Feynman-diagram calculation have been applied in [44].

Here we will follow the method based on colour-ordered amplitudes. In this approach the colour information is factorised from gauge-invariant purely kinematic pieces, the latter being embodied in primitive amplitudes [18]. Intermediate steps of the computation are then free of any colour information. This information is processed separately and reincorporated at the end of the calculation. As yet this approach is the only one which has led to phenomenological applications with five final state objects [11, 12]. However, one technical issue with the ordered approach is that the decomposition of matrix elements, and in particular the virtual piece, in terms of primitive amplitudes, can be non-trivial, especially as the number of fermion lines increases. The central difficulty is that the flow of quarks through a colour-ordered diagram is not uniquely determined by the external colour charges; each quark may navigate the loop in two distinct ways. In addition, the  $1/N_c$  terms in the gluon propagator do not cancel when exchanged between quark lines, as they do in the purely gluonic case. In this paper we show how the derivation of the colour decomposition can be automated using Feynman diagrams. This only needs to be done once for a given process, and is therefore not an issue for the numerical efficiency of an NLO program.

At leading order in the number of colours, the decomposition in terms of primitives is in general straightforward to write down. The corresponding results at subleading colour are non-trivial to derive, in particular, when multiple quark lines are present; up to now they have been dealt with on a case-by-case basis [19, 45–47]. Using our automated approach we will derive explicit expressions at fixed multiplicity for QCD amplitudes with many quark lines in terms of ordered objects. In particular, we present new results for the decomposition

of four- and six-quark amplitudes with up to seven coloured states. (See ancillary text files for our explicit expressions [56].) Thus we provide the missing pieces for the complete colour decomposition of QCD amplitudes with six and seven coloured states. These new results are of much wider relevance, however. With the colour decomposition of the pure QCD amplitudes at hand one can obtain rather simply their generalisations to include additional colourless objects such as leptons, vector bosons and Higgs bosons.

As a state-of-the-art application of our results we present distributions of the virtual contribution to  $W + 4$ -jet production including subleading-colour terms. A study at the LHC of this process has been published in ref. [11]. In that study the finite part of the virtual piece was given at leading order in a large- $N_c$  colour expansion. Here we confirm that the contribution of subleading-colour terms is small (a few percent), and shifts the virtual contribution uniformly over phase space.

Finally, we discuss an additional result, that is certain relations among the set of multi-quark primitive amplitudes. These relations appear as a by-product of our method and originate in the antisymmetry of the colour stripped fermion-fermion-gluon vertex. While manifest at low multiplicity, these “fermion-flip” relations become more and more intricate as coloured states are added. From a practical point of view, such relations enable us to express one-loop amplitudes in different ways. This can be exploited to obtain a minimal set of contributing ordered amplitudes, allowing a reduction of the computing resources needed for NLO calculations.

The organisation of this article is as follows. We begin in section II by describing in detail our conventions for dealing with the colour degrees of freedom. In section III we describe our algorithm and some details of our calculation. We also discuss how relations between primitive amplitudes are obtained as a by-product. In section IV we present selected results and a numerical study of the virtual contribution to  $W + 4$ -jet production. Finally, we draw our conclusions and present an outlook for future research.

## II. COLOUR DECOMPOSITION

In this section we review how full QCD one-loop amplitudes can be decomposed into contributions associated with  $SU(N_c)$  colour structures. While some of the notation extends the current literature, most notation and concepts follow the detailed discussions in [16, 18,

19] and the reviews [48, 49]. (See also ref. [50] for a recent review with topics related to this subject.)

### A. Basic conventions

We will be concerned with QCD scattering amplitudes of multiple quarks and gluons. Quarks are denoted by  $q$  and  $\bar{q}$  and are assumed to transform in the fundamental  $N_c$  and anti-fundamental  $\bar{N}_c$  representations of the gauge group  $SU(N_c)$ . When multiple quark flavours appear<sup>1</sup>, they will be distinguished by a flavour index  $q_l$  and  $\bar{q}_l$  with  $l = 1, 2, \dots, n_f$ . In the absence of this index, the quarks  $q$  and  $\bar{q}$  are understood to have a flavour number of one. We will keep the rank  $N_c$  as a free parameter and specialize to  $N_c = 3$  only for the numerical results. The colour indices of quarks and anti-quarks are denoted by  $\{i, j, \dots\}$  and  $\{\bar{i}, \bar{j}, \dots\}$  respectively. Gluons will be denoted by  $g$  with adjoint colour indices labelled by  $a, b, c$ , etc.

It will be convenient to consider also fermions in the adjoint representation of the gauge group. These will be denoted by capital letters  $Q$  and  $\bar{Q}$  and, in analogy to the fundamental fermions above, by  $Q_l$  and  $\bar{Q}_l$  with an explicit flavour label. The distinction of fermions and anti-fermions is then induced from the flavour charge. As above the fermions  $Q$  and  $\bar{Q}$  are understood as flavour one states, serving as a shorthand notation for  $Q_1$  and  $\bar{Q}_1$ .

### B. Colour algebra

The aim of the colour decomposition is to disentangle colour and kinematic degrees of freedom. This leads to a reorganization of scattering amplitudes in terms of ordered subamplitudes, which are typically easier to compute than the full amplitude itself. In addition, colour decomposition gives control over the interplay of colour and kinematic degrees of freedom. This can be used, for example, for the expansion of scattering amplitudes in terms of powers of the rank,  $N_c$ , of the gauge group  $SU(N_c)$ . Such an expansion can be exploited for efficiency gains [5, 26] in numerical NLO computations.

---

<sup>1</sup> We will consider only amplitudes with strictly different quark flavours. The cases with identical quarks are easily obtained as linear combinations of these.

In a Feynman-diagram representation of a scattering amplitude, gluon interactions are proportional to the structure constants  $f^{abc}$  of the gauge group,

$$[T^a, T^b] = i\sqrt{2} f^{abc} T^c, \quad (2.1)$$

where  $T^a$  are the Lie algebra generators in the fundamental representation, normalised such that  $\text{Tr}(T^a T^b) = \delta^{ab}$ . The quark-gluon interactions carry the fundamental representation generators  $(T^a)_i^{\bar{j}}$ .

We seek a uniform way of treating adjoint and fundamental colour indices, allowing the identification of common group theory factors. To this end we re-write all colour factors in terms of fundamental representation generators  $(T^a)_i^{\bar{j}}$  using

$$f^{abc} = -\frac{i}{\sqrt{2}} \text{Tr}([T^a, T^b] T^c). \quad (2.2)$$

Contracted adjoint indices can be reduced using the Fierz identity,

$$\sum_a (T^a)_k^{\bar{i}} (T^a)_l^{\bar{j}} = \delta_k^{\bar{j}} \delta_l^{\bar{i}} - \frac{1}{N_c} \delta_k^{\bar{i}} \delta_l^{\bar{j}}. \quad (2.3)$$

All group theory factors can then be written in a canonical way in terms of combinations of basic group theory data: powers of  $N_c$ , traces  $\text{Tr}(T^{a_1} T^{a_2} \dots T^{a_k})$ , generator strings  $(T^{a_1} T^{a_2} \dots T^{a_k})_i^{\bar{j}}$  and Kronecker deltas  $\delta_i^{\bar{j}}$ . No repeated adjoint indices appear, as they are all reduced using the Fierz identity (2.3).

Within generic formulae, when labels take boundary values, it is useful to adopt a slightly unconventional notation to keep expressions simple. A typical case that appears is a colour structure,  $(T^{a_1} T^{a_2} \dots T^{a_k})_i^{\bar{j}}$  with  $k \rightarrow 0$ . The natural interpretation for this is to replace this colour structure by a Kronecker delta,

$$(T^{a_1} T^{a_2} \dots T^{a_k})_i^{\bar{j}} \rightarrow \delta_i^{\bar{j}} \quad \text{for } k = 0. \quad (2.4)$$

Similarly, two boundary cases appear for traces of  $SU(N_c)$  generators,

$$\text{Tr}(T^{a_1} T^{a_2} \dots T^{a_k}) \rightarrow \text{Tr}(T^{a_1}) = 0 \quad \text{for } k = 1, \quad (2.5)$$

$$\text{Tr}(T^{a_1} T^{a_2} \dots T^{a_k}) \rightarrow 1 \quad \text{for } k = 0. \quad (2.6)$$

One might find the replacement  $\text{Tr}(T^{a_1} T^{a_2} \dots T^{a_k}) \rightarrow \text{Tr}(1) = N_c$  more natural for  $k = 0$ , however, we prefer to absorb factors of  $N_c$  into the definition of other objects, i.e. the partial amplitudes as defined below in section II C.

The above replacement rules (2.4), (2.5) and (2.6) will be understood implicitly throughout the present article.

### C. Partial amplitudes

Grouping terms of scattering amplitudes according to their colour structure gives their decomposition into partial amplitudes. The latter are in one-to-one correspondence with the distinct colour structures that appear in a scattering amplitude. In this section we spell out the form of two-quark, four-quark and six-quark amplitudes, as they will be used in the later parts of the article. We consider these amplitudes for distinct quark flavours. The cases with identical quark flavours can be obtained by appropriate (anti-) symmetrization of quark labels and we will not state them explicitly.

The partial amplitudes associated with the generic colour structures,

$$\text{Tr}(T^{a_1} \dots T^{a_{j-1}}) (T^{a_{j+1}} \dots T^{a_{j+k-1}})_{i_j}^{\bar{i}_{j+k}} (T^{a_{j+k+2}} \dots T^{a_{j+k+l}})_{i_{j+k+1}}^{\bar{i}_{j+k+l+1}} \dots, \quad (2.7)$$

will be denoted by,

$$A_{n;j,k,l,\dots}(1, \dots, j-1; j_q, j+1, \dots, (j+k)_{\bar{q}_{f_1}}; (j+k+1)_{q_2}, j+k+2, \dots, (j+k+l+1)_{\bar{q}_{f_2}}; \dots), \quad (2.8)$$

mimicking the index structure of the colour traces and generator strings. As usual, legs without particle subscripts are taken to be gluons. The variables  $f_i$  take values within the set  $\{1, \dots, n_f\}$  according to the flavour arrangement of the quarks. At tree level fewer colour structures appear; the single colour trace is absent if at least one quark pair is present. The indices  $j$  and  $k, l, \dots$  specify the size of colour traces and generator strings, respectively.

Partial amplitudes have symmetry properties implied by the colour structures. This includes a cyclic symmetry under rotation of gluons in a colour trace,

$$A_{n;j,\dots}(1, 2, \dots, j-1; \dots) = A_{n;j,\dots}(2, \dots, j-1, 1; \dots), \quad (2.9)$$

where we rotated the gluon indices associated with the colour trace. The full symmetry group generated by this operation is  $\mathbb{Z}_{j-1}$ . Similarly, the order in which the colour structures,  $(T^{a_m} \dots T^{a_n})_j^{\bar{i}}$ , appear leaves the value of the partial amplitudes invariant,

$$A_{n;j,k,l,\dots}(\dots; j_q, \dots, (j+k)_{\bar{q}_{f_1}}; (j+k+1)_{q_2}, \dots, (j+k+l+1)_{\bar{q}_{f_2}}; \dots) = \quad (2.10)$$

$$A_{n;j,l,k,\dots}(\dots; (j+k+1)_{q_2}, \dots, (j+k+l+1)_{\bar{q}_{f_2}}; j_q, \dots, (j+k)_{\bar{q}_{f_1}}; \dots),$$

and similarly for the exchange of other combinations of quark pairs.

Explicit decomposition of scattering amplitudes into partial amplitudes will be given in the following.

### 1. Two-quark partial amplitudes

At tree level the two-quark QCD amplitude [14, 15, 51–54] is

$$\mathcal{A}_n^{\text{tree}}(1_q, 2_{\bar{q}}, 3, \dots, n) = \sum_{\sigma \in S_{n-2}} (T^{a_{\sigma(3)}} \dots T^{a_{\sigma(n)}})_{i_1}^{\bar{i}_2} A_n^{\text{tree}}(1_q, \sigma(3), \dots, \sigma(n), 2_{\bar{q}}), \quad (2.11)$$

where  $S_{n-2}$  denotes the permutation group of  $n-2$  gluon labels with the amplitudes  $A_n^{\text{tree}}$  the tree level partial amplitudes. The elements of the permutation group  $\sigma$  are used in a two-fold way. On the one hand as a permuted list of gluon labels and, on the other hand, as functions,  $\sigma(k)$ , specifying the map of a given gluon, here gluon  $k$ , under the permutation  $\sigma$ . The colour structures here consist of a string of fundamental generators, terminated with the indices of the quark and anti-quark. We suppress the coupling constants here and throughout this paper.

At one-loop level the colour decomposition into partial amplitudes was given for all gluon multiplicities in ref. [18]. In addition to the tree-level colour structures, colour traces appear,

$$\begin{aligned} \mathcal{A}_n(1_q, 2_{\bar{q}}, 3, \dots, n) = & \quad (2.12) \\ & \sum_{j=1}^{n-1} \sum_{\sigma \in S_{n-2}/S_{(n-2;j)}} \text{Tr}(T^{a_{\sigma(3)}} \dots T^{a_{\sigma(j+1)}}) (T^{a_{\sigma(j+2)}} \dots T^{a_{\sigma(n)}})_{i_1}^{\bar{i}_2} \\ & \times A_{n;j}(\sigma(3), \dots, \sigma(j+1); 1_q, \sigma(j+2), \dots, \sigma(n), 2_{\bar{q}}). \end{aligned}$$

The sum in eq. (2.12) runs over all distinct colour structures. This is achieved by a double sum. The outer sum runs over the group theory structures and, within each of these, the inner sum runs over independent gluon orderings. Given the cyclic symmetry of the colour traces  $\text{Tr}(T^{a_{\sigma(3)}} \dots T^{a_{\sigma(j+1)}})$ , the full permutation group  $S_{n-2}$  of the  $n-2$  gluons is reduced by the cyclic subgroups  $S_{(n-2;j)} \equiv \mathbb{Z}_{j-1}$  that leave the traces in (2.12) invariant. We adopt here the notation in eqs. (2.4) and (2.5) for the boundary cases  $j = n-1$  and  $j = 1$ , respectively.

### 2. Four-quark partial amplitudes

We can follow analogous steps for amplitudes with two pairs of (distinct-flavour) quarks. Starting from a Feynman-diagram representation of a  $(q_1 \bar{q}_1 q_2 \bar{q}_2 g \dots g)$  amplitude, repeated application of eqs. (2.2) and (2.3) leads to the colour decomposition in terms of partial amplitudes.



It is convenient to give the explicit form of the tree amplitudes for four quarks and  $n$  gluons [15, 51, 54, 55],

$$\begin{aligned} \mathcal{A}_n^{\text{tree}}(1_{q_1}, 2_{\bar{q}_1}, 3_{q_2}, 4_{\bar{q}_2}; 5, \dots, n) = & \quad (2.13) \\ & \sum_{k=1}^{n-3} \sum_{\pi \in P_2} \sum_{\sigma \in S_{n-4}} (T^{a_{\sigma(5)}} \dots T^{a_{\sigma(k+3)}})_{i_{\pi(1)}}^{\bar{i}_2} (T^{a_{\sigma(k+4)}} \dots T^{a_{\sigma(n)}})_{i_{\pi(3)}}^{\bar{i}_4} \\ & \times A_{n;k}^{\text{tree}}(\pi(1_{q_1}), \sigma(5), \dots, \sigma(k+3), 2_{\bar{q}_1}; \pi(3_{q_2}), \sigma(k+4), \dots, \sigma(n), 4_{\bar{q}_2}). \end{aligned}$$

For the boundary cases  $k = 1$  and  $k = n - 3$  the colour structures  $(T^{a_{\sigma(5)}} \dots T^{a_{\sigma(k+3)}})_{i_{\pi(1)}}^{\bar{i}_2}$  and  $(T^{a_{\sigma(k+4)}} \dots T^{a_{\sigma(n)}})_{i_{\pi(3)}}^{\bar{i}_4}$  have to be replaced by  $\delta_{i_{\pi(1)}}^{\bar{i}_2}$  and  $\delta_{i_{\pi(3)}}^{\bar{i}_4}$  respectively (see section II A).  $P_2$  stands for the permutation group of the quarks  $\{1_{q_1}, 3_{q_2}\}$ . In an overloaded notation, the elements  $\pi \in P_2$  are also interpreted as maps on the quarks and quark labels, e.g. the notation  $\pi(1_{q_1})$  and  $\pi(1)$  is used to denote mappings of quark and quark label, respectively. The signs keeping track of the sign in the  $(-1/N_c)$ -term (see eq. (2.3)) in the colour-octet projector of the gluon propagator are pulled into the definition of the partial amplitudes in terms of colour-ordered tree amplitudes. Details can be found in the supplied data files as described in section IV B.

At one-loop level a similar colour decomposition into partial amplitudes gives [45–47],

$$\begin{aligned} \mathcal{A}_n(1_{q_1}, 2_{\bar{q}_1}, 3_{q_2}, 4_{\bar{q}_2}; 5, \dots, n) = & \\ & \sum_{\substack{j=1, n-3 \\ k=1, n-(j+2)}} \sum_{\pi \in P_2} \sum_{\sigma \in S_{n-4}/S_{(n-4;j)}} \text{Tr}(T^{a_{\sigma(5)}} \dots T^{a_{\sigma(j+3)}}) \\ & \times (T^{a_{\sigma(j+4)}} \dots T^{a_{\sigma(j+2+k)}})_{i_{\pi(1)}}^{\bar{i}_2} (T^{a_{\sigma(j+3+k)}} \dots T^{a_{\sigma(n)}})_{i_{\pi(3)}}^{\bar{i}_4} \\ & \times A_{n;j,k}(\sigma(5, j+3); \pi(1_{q_1}), \sigma(j+4, j+2+k), 2_{\bar{q}_1}; \pi(3_{q_2}), \sigma(j+3+k, n), 4_{\bar{q}_2}), \end{aligned} \quad (2.14)$$

where we again use the conventions for the boundary cases given in section II A. We also introduced the abbreviation  $\sigma_{(i,j)} = \{\sigma(i), \sigma(i+1), \dots, \sigma(j-1), \sigma(j)\}$ .

### 3. Six-quark partial amplitudes

We now consider amplitudes with three distinct quark flavours. Starting from a Feynman-diagram representation of a  $(q_1 \bar{q}_1 q_2 \bar{q}_2 q_3 \bar{q}_3 g \dots g)$  amplitude, repeated application of eqs. (2.2) and (2.3) once again leads to the colour decomposition in terms of partial amplitudes. For simplicity of exposition we give the six-quark and seven-quark one-gluon partial amplitudes.

The explicit form of the tree amplitudes for six quarks is given by [15, 51, 54],

$$\begin{aligned} \mathcal{A}_6^{\text{tree}}(1_{q_1}, 2_{\bar{q}_1}, 3_{q_2}, 4_{\bar{q}_2}, 5_{q_3}, 6_{\bar{q}_3}) &= \sum_{\pi \in P_3} \delta_{i_{\pi(1)}}^{\bar{i}_2} \delta_{i_{\pi(3)}}^{\bar{i}_4} \delta_{i_{\pi(5)}}^{\bar{i}_6} \\ &\times A_{6;1,1}^{\text{tree}}(\pi(1_{q_1}), 2_{\bar{q}_1}; \pi(3_{q_2}), 4_{\bar{q}_2}; \pi(5_{q_3}), 6_{\bar{q}_3}), \end{aligned} \quad (2.15)$$

with  $P_3$  the permutation group of the quarks  $\{1_{q_1}, 3_{q_2}, 5_{q_3}\}$ .

For one-loop amplitudes a similar colour decomposition into partial amplitudes gives,

$$\begin{aligned} \mathcal{A}_6(1_{q_1}, 2_{\bar{q}_1}, 3_{q_2}, 4_{\bar{q}_2}, 5_{q_3}, 6_{\bar{q}_3}) &= \sum_{\pi \in P_3} \delta_{i_{\pi(1)}}^{\bar{i}_2} \delta_{i_{\pi(3)}}^{\bar{i}_4} \delta_{i_{\pi(5)}}^{\bar{i}_6} \\ &\times A_{6;1,1,1}(\pi(1_{q_1}), 2_{\bar{q}_1}; \pi(3_{q_2}), 4_{\bar{q}_2}; \pi(5_{q_3}), 6_{\bar{q}_3}). \end{aligned} \quad (2.16)$$

The generalization of the above colour decompositions (2.16) to seven-point partial amplitudes is given by,

$$\begin{aligned} \mathcal{A}_7(1_{q_1}, 2_{\bar{q}_1}, 3_{q_2}, 4_{\bar{q}_2}, 5_{q_3}, 6_{\bar{q}_3}; 7) &= \sum_{\sigma \in \mathbb{Z}_3} \sum_{\pi \in P_3} (T^{a_7})_{i_{\pi(1)}}^{\bar{i}_{\sigma(2)}} \delta_{i_{\pi(3)}}^{\bar{i}_{\sigma(4)}} \delta_{i_{\pi(5)}}^{\bar{i}_{\sigma(6)}} \\ &\times A_{7;1,2,1}(\pi(1_{q_1}), 7, \sigma(2_{\bar{q}_1}); \pi(3_{q_2}), \sigma(4_{\bar{q}_2}); \pi(5_{q_3}), \sigma(6_{\bar{q}_3})). \end{aligned} \quad (2.17)$$

The cyclic group  $\mathbb{Z}_3$  is understood to rotate the three quarks  $\{1_{q_1}, 3_{q_2}, 5_{q_3}\}$  in order to guarantee that the gluon is emitted from all quark sources. Refined definitions of various elements in eq. (2.17) follow conventions in eq. (2.15).

Tree amplitudes take an analogous form, as was the case for the 6-point formulas (2.16) and (2.15), so we do not state the tree-level formula here explicitly.

## D. Primitive amplitudes

Partial amplitudes can be further expressed as linear combinations of ‘primitive amplitudes’ [18]. In fact, primitive amplitudes are defined as a set of gauge-invariant, colour-ordered building blocks which suffice to express a given set of partial amplitudes. We discuss in this subsection how to characterize and generate primitive amplitudes. Our algorithm for expressing partial amplitudes in terms of primitive amplitudes will be given in section III.

Primitive amplitudes can be specified by sets of adjoint representation colour-ordered Feynman diagrams [18, 49]. These diagrams differ from the standard Feynman diagrams in that colour labels are dropped. At gluon vertices, for example, the structure constants  $f^{abc}$  are omitted. Gluon vertices dressed with colour labels are symmetric under the exchange of

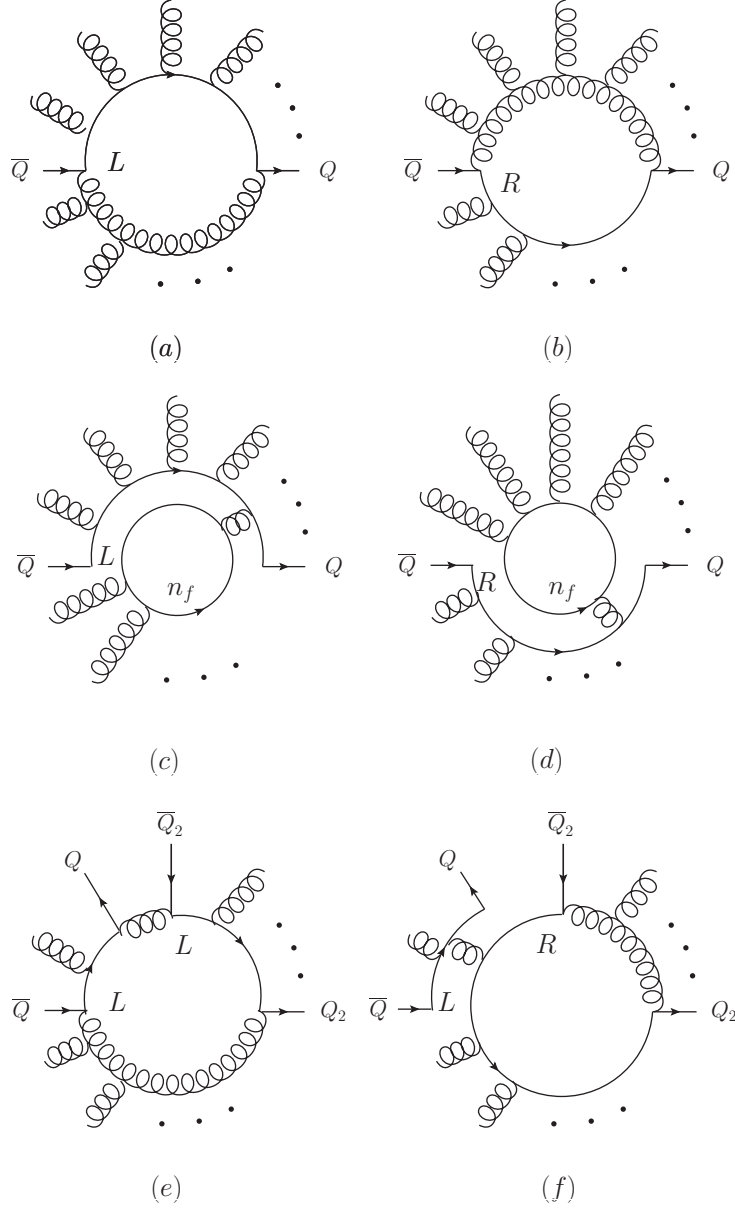


FIG. 1: Parent diagrams with a distinct routing of quark lines: (a) a parent with a ‘left-turner’ fermion labelled by ‘ $L$ ’, (b) a ‘right-turner’ fermion, labelled by ‘ $R$ ’, (c) ‘ $n_f$ -left-turner’ ( $n_fL$ ) fermions, (d) ‘ $n_f$ -right-turner’ ( $n_fR$ ) fermions. Two routing labels are associated to the distinct quark flavours  $Q$  and  $Q_2$ : (e) ‘left-left-turner’ ( $LL$ ) fermions, (f) ‘left-right-turner’ ( $LR$ ) fermions. Note that in (f) the first fermion does not in fact enter the loop. In general as many  $L/R$ -labels appear as there are distinct external quark flavours. Quarks are associated with capital letter  $Q$ ’s, as in primitive amplitudes they arise from adjoint representation colour assignments in our algorithm.

legs. Due to the anti-symmetry of the structure constants  $f^{abc}$ , the remaining kinematic part is necessarily anti-symmetric under exchange of legs. In colour-ordered Feynman diagrams one must preserve the ordering of the external legs to keep track of the signs associated with the vertices. Given a set of colour-ordered Feynman diagrams one uses colour-ordered Feynman rules (see e.g. [48]) to obtain amplitudes and eventually primitive amplitudes.

We require the set of all primitive amplitudes needed to compute a given scattering amplitude. In particular, we will need their representation in terms of sets of Feynman diagrams. This may be generated systematically in two steps, which we will describe in full below:

1. generate ‘coarse’ primitive amplitudes,
2. split the coarse primitives according to the routing of fermions around the loop.

The coarse primitives can be thought of as sums of planar, ordered diagrams, obtained using colour-ordered Feynman rules. Each coarse primitive amplitude corresponds to a particular ordering of the external legs.

In practise, we obtain the coarse primitive amplitudes starting from a colour-dressed representation of the amplitude by taking all partons, including quarks, in the adjoint representation of the gauge group. Performing all the colour algebra reductions, one finds a set of terms, some with single and some with double traces of fundamental generators, just as is the case for purely gluonic amplitudes. The coarse primitive amplitudes

$$A^{\text{coarse}}(1, \dots, Q_1, \dots, \overline{Q}_1 \dots), \quad (2.18)$$

are then identified as the coefficients of the single trace structures

$$N_c \text{Tr}(T^{a_1} \dots T^{a_{Q_1}} \dots T^{a_{\overline{Q}_1}} \dots). \quad (2.19)$$

Secondly, a finer splitup of the coarse primitive amplitudes into actual primitive amplitudes is obtained by analysing the fermions’ routing around the loop. This can be considered a generalisation of the familiar case of diagrams with a fermion circulating in the loop not mixing under gauge transformations with diagrams with a gluon in the loop. Similarly, fermion routing information in Feynman diagrams allows to split coarse primitive amplitudes into finer gauge-invariant subsets. The routing information of a fermion line specifies whether the fermion turns left or right upon entering the loop. In the case where the fermion

does not enter the loop, the left/right label is assigned according to which side of the loop the fermion passes. We follow the fermion line starting from the anti-quark. In this way, each fermion line is labelled as a left- or right-turner, denoted by capital labels  $L$  and  $R$ , respectively. Some examples can be found in fig. 1.

Algorithmically, the routing information of a colour-ordered Feynman diagram can be determined by cutting a single loop propagator. If no gluon propagator is available, the Feynman diagram has to correspond to an  $n_f$  term. We then cut the internal fermion line. If a gluon loop-propagator is available we instead cut that one. After cutting the propagator the Feynman diagram corresponds to a diagram of a colour-ordered tree amplitude. The fermion routing information is then in one-to-one correspondence to the ordering of external fermions relative to their anti-fermions and may be read off directly. The coarse primitive amplitudes can then be sorted diagram by diagram into the finer classes of primitive amplitudes with definite fermion flow.

The explanation of the gauge invariance of the primitive amplitudes as defined above has been given in ref. [18]. The basic reasoning relies on a non-standard colour charge assignment to quarks and gluons. Primitive amplitudes of standard QCD can typically be interpreted as partial amplitudes of a theory with non-standard gauge groups and colour charges. Gauge invariance of a class of Feynman amplitudes is then ensured from the associated gauge invariance of partial amplitudes. The non-standard colour assignments include various bifundamental and adjoint representations in product gauge groups  $SU(N_1) \times SU(N_2) \times SU(N_3) \dots$  for quarks and gluons respectively. The basic logic is only a minor generalisation of that presented in the original literature [18], to which we refer for further details.

### 1. Notation

Pictorially, primitive amplitudes can be characterized by a small set of ‘parent’ Feynman diagrams. These are the representative colour-ordered Feynman diagrams of a primitive amplitude with the maximal number of loop propagators. An additional requirement is that the complete set of Feynman diagrams associated with a primitive amplitude can be obtained from the parent diagrams through pinching of propagators and ‘pulling out’ of tree amplitudes.

Example parent diagrams of six distinct primitive amplitudes are shown in fig. 1. The

diagrams are representative of classes of colour-ordered Feynman diagrams. Parent diagrams (a), (b), (c) and (d) have identical external states, as do diagrams (e) and (f). They differ by the routing of the fermion lines around the loop and are gauge invariant individually<sup>2</sup>. The routing information of the fermions is given in terms of left- and right-turner labels;  $L$  and  $R$ . Closed fermion loops are specified by an additional label  $n_f$ . Such routing labels must be specified for each fermion line.

So instead of specifying a primitive amplitude by the set of colour-ordered Feynman diagrams contributing to it, we can be more concise, and specify only 1) an ordered set of external states and 2) routing data of fermion lines.

We will use this information to specify primitive amplitudes. In our conventions, for the amplitudes shown in fig. 1 we will use the following notation,

$$\begin{aligned}
(a) : & \quad A^L(Q, \dots g, g, \overline{Q}, g, g, g, g, \dots), \\
(b) : & \quad A^R(Q, \dots g, g, \overline{Q}, g, g, g, g, \dots), \\
(c) : & \quad A^{n_f L}(Q, \dots g, g, \overline{Q}, g, g, g, g, \dots), \\
(d) : & \quad A^{n_f R}(Q, \dots g, g, \overline{Q}, g, g, g, g, \dots), \\
(e) : & \quad A^{LL}(Q, \overline{Q}_2, g, Q_2, \dots g, g, \overline{Q}, g, \dots), \\
(f) : & \quad A^{LR}(Q, \overline{Q}_2, g, Q_2, \dots g, g, \overline{Q}, g, \dots).
\end{aligned}$$

Fermion lines will be given ascending flavour numbers starting from 1 (we identify  $Q \equiv Q_1$ ). The routing information will be specified by a list of labels  $L$ ,  $R$ .  $L$  stands for a fermion that turns left upon approaching the loop, while  $R$  stands for a right turning fermion. The first label in the list corresponds to the first flavour-line, the second label to the second line etc. Closed fermion loops are indicated by an additional label  $n_f$ . External states are given in clockwise order and we exploit the rotational symmetry (described in the next section) to rotate quarks with flavour one into the first position.

## 2. Symmetry properties

Pure-QCD primitive amplitudes enjoy a variety of symmetries. These are useful for reducing the number of independent primitive amplitudes that need to be computed. We

---

<sup>2</sup> More precisely, the primitive amplitudes they correspond to are gauge-invariant.

use the symmetries below to write primitives in a standard form starting with a left-turner label, with the quark of flavour one in the first position of the particle labels,

$$A^{L\cdots}(Q, \dots) \quad \text{or} \quad A^{n_f L\cdots}(Q, \dots). \quad (2.20)$$

The relevant symmetry transformations are described below. In addition, an extended set of relations between primitive amplitudes will be discussed below in 3.10.

First of all, cyclic rotation of the labels does not change the primitive amplitudes,

$$A^{\cdots}(1, 2, \dots, n) = A^{\cdots}(2, \dots, n, 1). \quad (2.21)$$

Another symmetry arises from flipping over the colour-ordered diagrams of a given primitive. This reverses the ordering of the external states and exchanges all left- and right-turners up to a sign. In the case of a two quark line amplitude we have,

$$\begin{aligned} A^{LR}(1_q, 2, \dots, k_{\bar{q}}, \dots, l_{q_2}, \dots, m_{\bar{q}_2}, \dots, n) = \\ (-1)^n A^{RL}(1_q, n, \dots, m_{\bar{q}_2}, \dots, l_{q_2}, \dots, k_{\bar{q}}, \dots, 2). \end{aligned} \quad (2.22)$$

A further generic relation between primitive amplitudes originates in the reversal of a fermion's arrow. This leads to a flip of the routing label,

$$A^{\cdots L_i \cdots}(\dots, k_{q_i}, \dots, l_{\bar{q}_i}, \dots, n) = A^{\cdots R_i \cdots}(\dots, k_{\bar{q}_i}, \dots, l_{q_i}, \dots, n). \quad (2.23)$$

This property is naturally generalised to the case with multiple quark lines. Each quark line may be reversed and the associated turner label flipped,  $L \leftrightarrow R$ . We will not use this transformation here, preferring to keep the distinction between quarks and anti-quarks.

## E. Colour decomposition of partial amplitudes.

In this section we present our notation for partial amplitudes given as linear combinations of primitives. As the expressions are lengthy we prefer to write them in a simplified form, which is also more convenient for use with a computer program. We display only a small sample in the main body of this paper, and attach the remainder as text files [56]. Additional information concerning the supplied data-files can be found below in section IV B.

To explain our notation we refer to fig. 2 where we show our result for the four quark amplitude. The line starting with ‘\* Partial’ indicates the beginning of the expression

and is followed by a specification of which particular partial amplitude is being considered. The notation for this mimics the argument of the partial amplitudes (2.8). It takes the form of a comma separated list with each element of the list denoting an  $SU(N_c)$  colour structure. Such a colour structure is unambiguously specified by a list of particles. Quarks in the fundamental representation are denoted by  $q$ , and may have an additional numerical label to distinguish different flavours ( $q, q2, q3 \dots$ ). Anti-quarks are written  $qb, qb2, qb3$  etc. Momentum labels appear in parentheses, e.g.  $q(1)$  denotes a quark that carries the momentum  $k_1$ . For the case of fig. 2, the colour structure is  $\delta_{i_1}^{\bar{i}_2} \delta_{i_3}^{\bar{i}_4}$ .

There follows specification of the born contribution to this partial amplitude in terms of colour-ordered tree-level amplitudes. The line starting with the label,

$$\begin{aligned} \text{born} \quad & \{ \dots | \dots \\ & \dots | \dots \\ & \text{etc.} \\ & \} \end{aligned}$$

shows a list of particles in the adjoint representation and, separated by a vertical line, '|', the coefficient of the given tree within the partial amplitude. Labels with capital letters  $Q, Q2$  etc. are used for these kind of quarks. For partial amplitudes that are a linear combination of colour-ordered tree amplitudes, multiple line entries are used, each displaying a list of particle labels and the weight of the associated tree amplitude within the partial amplitude.

In more conventional form the four quark born amplitude is given by,

$$\mathcal{A}_4^{\text{tree}}(1_q, 2_{\bar{q}}, 3_{q_2}, 4_{\bar{q}_2}) = A^{\text{tree}}(1_Q, 2_{\bar{Q}}, 3_{Q_2}, 4_{\bar{Q}_2}) \times \left( \delta_{i_1}^{\bar{i}_2} \delta_{i_3}^{\bar{i}_4} - \frac{1}{N_c} \delta_{i_1}^{\bar{i}_2} \delta_{i_3}^{\bar{i}_4} \right). \quad (2.24)$$

```
* Partial: { q(1) qb(2) , q2(3) qb2(4) }

born { Q(1) Qb(2) Q2(3) Qb2(4) | (-1/Nc) }
loop {
  LL | Q(1) Qb2(4) Q2(3) Qb(2) | 1/Nc^2
  LR | Q(1) Q2(3) Qb2(4) Qb(2) | 1/Nc^2 + 1
  LR | Q(1) Qb2(4) Q2(3) Qb(2) | 1/Nc^2
  LL | Q(1) Qb(2) Qb2(4) Q2(3) | -1/Nc^2
  nfLL | Q(1) Qb2(4) Q2(3) Qb(2) | -nf/Nc
}
```

FIG. 2: Four quark partial amplitude decomposed into primitive amplitudes, in the notation of the attached file.



The displayed partial amplitude corresponds to the second term in eq. (2.24) and the ordered born amplitude is  $A^{\text{tree}}(1_Q, 2_{\overline{Q}}, 3_{Q_2}, 4_{\overline{Q}_2})$  weighted by a factor of  $-\frac{1}{N_c}$ .

The remaining entries specify the one-loop partial amplitude in terms of primitives. This entry starts with the header ‘*loop*’,

$$\begin{aligned} \text{loop} \quad \{ \\ & \dots | \dots | \dots \\ & \dots | \dots | \dots \\ & \text{etc.} \\ \} \end{aligned}$$

with the individual lines each specifying the turner labels, an ordered list of external states and the weight of the primitive amplitude. In total this represents a sum of primitive amplitudes, each with a  $N_c$ - and/or  $n_f$ -dependent coefficient. For the present example, displayed in fig. 2, the partial amplitude is given by,

$$\mathcal{A}_4(1_q, 2_{\overline{q}}, 3_{q_2}, 4_{\overline{q}_2}) = \dots + A_{4;1,1}(1_q, 2_{\overline{q}}; 3_{q_2}, 4_{\overline{q}_2}) \delta_{i_1}^{\tilde{i}_2} \delta_{i_3}^{\tilde{i}_4} + \dots, \quad (2.25)$$

$$\begin{aligned} A_{4;1,1}(1_q, 2_{\overline{q}}; 3_{q_2}, 4_{\overline{q}_2}) &= \frac{1}{N_c^2} A^{LL}(1_Q, 4_{\overline{Q}_2}, 3_{Q_2}, 2_{\overline{Q}}) + \left(1 + \frac{1}{N_c^2}\right) A^{LR}(1_Q, 3_{Q_2}, 4_{\overline{Q}_2}, 2_{\overline{Q}}) \\ &+ \frac{1}{N_c^2} A^{LR}(1_Q, 4_{\overline{Q}_2}, 3_{Q_2}, 2_{\overline{Q}}) - \frac{1}{N_c^2} A^{LL}(1_Q, 2_{\overline{Q}}, 4_{\overline{Q}_2}, 3_{Q_2}) \\ &- \frac{n_f}{N_c} A^{n_f LL}(1_Q, 4_{\overline{Q}_2}, 3_{Q_2}, 2_{\overline{Q}}). \end{aligned} \quad (2.26)$$

The five primitive amplitudes appear in the same order as in fig. 2, where they are given on separate lines. Each primitive amplitude is specified by a list of particles in the adjoint representation and string of fermion left/right-turner labels. We denote adjoint quarks with a capital  $Q$ . Each quark line has a ‘turner label’  $L$  or  $R$ , which described the direction it turns upon approaching the loop, as described in section II D.

The above expression can be compared to the one given for the partial amplitude denoted by  $A_{6;2}$  in eq.(2.15) of ref. [19]. To simplify this comparison we set the number of scalars  $n_s = 0$  and drop the top-quark contributions in the expression for  $A_{6;2}$ . We can omit the colour-neutral lepton states, as they play no role in this colour decomposition. To match the expression for  $A_{6;2}$  with our eq. (2.26) we have to replace  $2 \leftrightarrow 4$  in the expression for  $A_{6;2}$ . We can then identify  $A^{+-}(1, 3, 4, 2) = A^{LR}(1, 3, 4, 2)$ ,  $A^{++}(1, 4, 3, 2) = A^{LL}(1, 4, 3, 2)$ ,

$A^{sl}(4, 3, 1, 2) = A^{LL}(1, 2, 4, 3) - A^{LR}(1, 4, 3, 2)$  and  $A^{s,++}(1, 4, 3, 2) + A^{f,++}(1, 4, 3, 2) = -A^{n_f LL}(1, 4, 3, 2)$ . (Compared to [19] we differ here by an overall sign in the definition of the  $n_f$ -terms, which introduces this apparent relative minus-sign.) This identification can also be inferred from comparison of parent diagrams. The relative minus sign in the expression for  $A^{sl}(4, 3, 1, 2)$  appears from the asymmetry of the fermion-fermion-gluon three-point vertex. Upon reversing the order of the quarks  $1_q$  and  $2_{\bar{q}}$  and rotation of the labels one finds the identity,  $-A^{LL}(1, 2, 4, 3) = A^{RL}(2, 1, 4, 3) = A^{RL}(1, 4, 3, 2)$ , with the relative minus sign absorbed into the re-ordering of external legs.

With this comparison we conclude the explanation of our conventions.

### III. COLOUR DECOMPOSITION ALGORITHM

In this section we will describe our setup for obtaining partial amplitudes in terms of primitive amplitudes, for arbitrary processes. The algorithm we use is based on analysing Feynman diagrams using their colour information. We identify partial amplitudes in terms of linear combinations of Feynman diagrams. Similarly, we express primitive amplitudes in terms of Feynman diagrams. Finally, we express partial amplitudes in terms of primitive amplitudes by solving the linear set of equations to eliminate the explicit dependence on the diagrams. In addition to the colour decomposition of the partial amplitudes, we find non-trivial relations between primitive amplitudes, which arise due to the redundancy of the linear equations we solve.

#### A. Setup

We begin by generating all one-loop Feynman diagrams using QGRAF [57]. We remove diagrams with contact terms (four-point gluon vertices), tadpoles and those with bubbles on external lines. Let us suppose there are  $N_d$  diagrams after this procedure. The output of this program is then processed using the computer algebra package FORM [58]. Using this package we dress the diagrams with colour - gluons in the adjoint and quarks in the fundamental representation of the gauge group - and simplify the colour algebra using eqs. (2.2) and (2.3). There is no need to substitute the kinematic parts of the Feynman rules, so we leave this information implicit. This procedure gives us an expression for the amplitude in

terms of sums of diagrams multiplied by the various colour structures that may appear,

$$\mathcal{A}(\{\mathbf{a}_g, \mathbf{i}_q\}) = \sum_{i=1}^{N_P} A_i^{\text{partial}} C_i(\{\mathbf{a}_g, \mathbf{i}_q\}). \quad (3.1)$$

On the left hand side is the fully colour-dressed amplitude, which depends on the set of colour charges  $\{\mathbf{a}_g, \mathbf{i}_q\}$  of the external particles. The right hand side is its decomposition in terms of  $N_P$  partial amplitudes  $A_i^{\text{partial}}$ , multiplying colour structures  $C_i$ . Partial amplitudes and their colour structures are discussed further in section II C. Here and in the following we leave implicit all dependence on momenta and helicities.

After processing the diagrams in this way, we find expressions for the  $A_i^{\text{partial}}$  as sums of diagrams,

$$A_i^{\text{partial}} = \sum_{j=1}^{N_d} K_i^j d_j \quad \text{for } i = 1, \dots, N_P. \quad (3.2)$$

Here  $K_i^j$  is a  $N_P \times N_d$  matrix which describes how the  $j$ 'th diagram contributes to the  $i$ 'th partial amplitude. The entries of the matrix  $K_i^j$  consist of simple functions of the rank of the gauge group,  $N_c$ . The  $d_i$  are the kinematic parts of the set of Feynman diagrams, but we will not need their explicit form here. It is sufficient to think of them as tags for the individual Feynman diagrams.

With this in hand, we now discuss how the primitive amplitudes are expressed in terms of diagrams. We first go back and dress the original one-loop Feynman diagrams with colour assuming that all external particles, including quarks, live in the adjoint representation of the gauge group. Upon simplifying the colour algebra, we find two types of term — those with single traces, and those with double traces, exactly as one finds for purely gluonic amplitudes,

$$\mathcal{A}^{\text{adjoint}}(\{\mathbf{a}_g, \mathbf{a}_q\}) = \sum_{\sigma \in S_n / \mathbb{Z}_n} N_c \text{Tr}(T^{a_{\sigma(1)}} T^{a_{\sigma(2)}} \dots T^{a_{\sigma(n)}}) A^{\text{coarse}}(\sigma) + \text{double trace terms}. \quad (3.3)$$

In this equation we have added the label ‘adjoint’ to remind the reader that this is the amplitude with all external particles in the adjoint representation. The sum is over the permutation group  $S_n$  of  $n$  elements modulo cyclic rotations  $\mathbb{Z}_n$ . Some permutations may not appear when fermion lines of the diagrams cannot be arranged in a planar way. We drop all double-trace terms. Note that there is no approximation being made here — this is simply the definition of the primitive amplitudes. (The double trace contributions can be fully reconstructed from the primitive amplitudes, though we will not need to do this here.)

If we were to restrict ourselves to the case of amplitudes with only adjoint particles, then we could now identify the coefficients  $A^{\text{coarse}}(1, 2, \dots, n)$  of the single trace structures as primitive amplitudes,

$$A_k^{\text{coarse}}(\sigma_k) = \sum_{j=1}^{N_d} (L^{\text{coarse}})_k^j d_j, \quad k = 1, \dots, N_{\text{prim}}^{\text{coarse}}, \quad (3.4)$$

where  $(L^{\text{coarse}})_k^j$  is a coefficient matrix with integer entries.

However, as described in section IID, following ref. [18] for the case of a single fermion line, when fundamental quarks are present these objects can be split further into finer gauge invariant pieces. These pieces are distinguished by the direction of the fermion line relative to the loop. Following the fermion line into the diagram, one defines ‘left-turner’ (L) fermions as those which pass to the left of the loop, while ‘right-turner’ (R) fermions pass to the right. If the loop is in fact a closed fermion loop, the diagram acquires an additional label  $n_f$ . These concepts have already been discussed in section IID. We extend this grouping of diagrams to generic processes by labelling each fermion line as a left- or right- turner. We thus take the primitive amplitudes to be

$$A^{D_1 \dots D_{N_q}}(1, \dots, n), \quad (3.5)$$

where  $N_q$  is the number of fermion lines and  $D_i \in \{L, R\}$  labels each as either a left or right turner. In the argument list we have suppressed the identities of the  $2N_q$  fermions and  $n - 2N_q$  gluons.

Let us suppose there are  $N_{\text{prim}}$  primitive amplitudes. Using our setup we derive an expression for each of them as a sum of diagrams, just as we did for the partial amplitudes in eq. (3.2),

$$A_k^{\mathbf{D}_k} \equiv A^{\mathbf{D}_k}(\sigma_k) = \sum_{j=1}^{N_d} L_k^j d_j, \quad k = 1, \dots, N_{\text{prim}} \quad (3.6)$$

where the direction labels are implied. Here  $L_k^j$  is a  $N_{\text{prim}} \times N_d$  matrix describing how the  $j$ 'th diagram contributes to the  $k$ 'th primitive.

We now attempt to express the partial amplitudes of eq. (3.2) as linear combinations of the primitive amplitudes of eq. (3.6). We write

$$A_i^{\text{partial}} = \sum_{k=1}^{N_{\text{prim}}} Z_i^k A_k^{\mathbf{D}_k}, \quad (3.7)$$

where  $i$  runs from 1 to  $N_P$ , and look for solutions for the coefficients  $Z_i^k$  of this set of linear equations,

$$K_i^j = Z_i^k L_k^j. \quad (3.8)$$

The solutions of this set of equations are typically not unique as will be discussed further in section III B.

We have confirmed that the solutions match those obtained from the known all-multiplicity expressions in ref. [17] in the case of purely gluonic processes, and ref. [18] for processes with one quark line. For processes with more than one quark line we reproduce the closed form analytic expressions available in refs. [19, 46] and [47]. Beyond that we are able to present new results as presented in more detail in section IV.

## B. Relations

The linear equations (3.8) typically give rise to non-trivial solutions  $\{(Z^{\text{rel}})^k\}$ ,

$$(Z^{\text{rel}})^k L_k^j = 0. \quad (3.9)$$

This means that the Feynman diagrams associated with a linear combination of primitive amplitudes add up to zero. Interpreted for the primitive amplitudes this implies linear relations,

$$0 = \sum_{k=1}^{N_{\text{prim}}} (Z_i^{\text{rel}})^k A_k^{\mathbf{D}_k}, \quad i = 1, \dots, N^{\text{relations}}, \quad (3.10)$$

for the case that  $N^{\text{rel}}$  solutions  $(Z_i^{\text{rel}})^k$  have been found. In order to verify the relations no detailed knowledge of the Feynman amplitudes is necessary. They arise at the diagrammatic level when taking into account the anti-symmetry of colour-ordered three-point vertices.

It is tempting to relate the above relations to the ones that are known for colour-ordered tree amplitudes, such as the  $U(1)$  decoupling identity [14, 52, 53] and non-abelian generalizations [21] through the Kleiss-Kuijf relations [59]. The role of these relations for loop-level colour-decomposition has already been pointed out some time ago [17, 27, 60] and recently reviewed in ref. [50]. We will not attempt a detailed analysis into this direction but make some general remarks about the observed relations (3.10).

One remark concerns the importance of having multiple fermion lines to obtain the above relations. When considering fermion lines the anti-symmetry of the fermion-fermion-gluon

three point vertex implies certain fermionic amplitudes may be related. The complete list of all relations is a by-product of our way to obtain the colour decompositions of partial amplitudes. By inspection we observed that the relations in eq. (3.10) originate from this anti-symmetry. We will discuss two examples below in section III B 1. As the multiplicity of quark amplitudes is increased by addition of gluons, the number of relations increases due to the different ways gluons can be added to ordered amplitudes. The new relations appear as descendants of the ones of the purely fermionic amplitudes.

A second remark is about an application of the above relations. For numerical evaluation of scattering amplitudes (see later in section IV) we exploit the relations between primitive amplitudes (3.10) to optimise caching and thus run-times. In the explicit expressions given, we pick methodically a subset of primitive amplitudes using the relations. In fact we sort primitive amplitudes according to the number of propagators of their parent diagrams. We then apply the relations to eliminate primitive amplitudes starting from the ones with the minimal number of parent propagators as part of the loop. This procedure minimizes the number of primitive amplitudes that need to be computed. However, it does not take into account which primitive amplitudes are most easily computed.

Similarly, one could make use mostly of primitive amplitudes with a minimal number of parent loop propagators. For a unitarity-based algorithm this choice would be beneficial, reducing the number of unitarity-cuts to consider. We leave a more thorough analysis of the relations between primitive amplitudes to the future. It seems likely that an understanding of the relations between primitive amplitudes (3.10) will be helpful towards establishing all- $n$  formulae for the colour decompositions, which are beyond the scope of the present article.

### 1. *Example Relations*

For the set of primitive amplitudes we are dealing with the origin of these relations are the symmetry properties of the quark-quark-gluon vertices. A simple example with an internal fermion line is given by,

$$A^{\text{n}_f\text{LL}}(1_Q, 5_{\overline{Q}_2}, 4_{Q_2}, 2, 3_{\overline{Q}}) + A^{\text{n}_f\text{LR}}(1_Q, 4_{Q_2}, 5_{\overline{Q}_2}, 2, 3_{\overline{Q}}) + A^{\text{n}_f\text{LL}}(1_Q, 5_{\overline{Q}_2}, 2, 4_{Q_2}, 3_{\overline{Q}}) = 0, \quad (3.11)$$

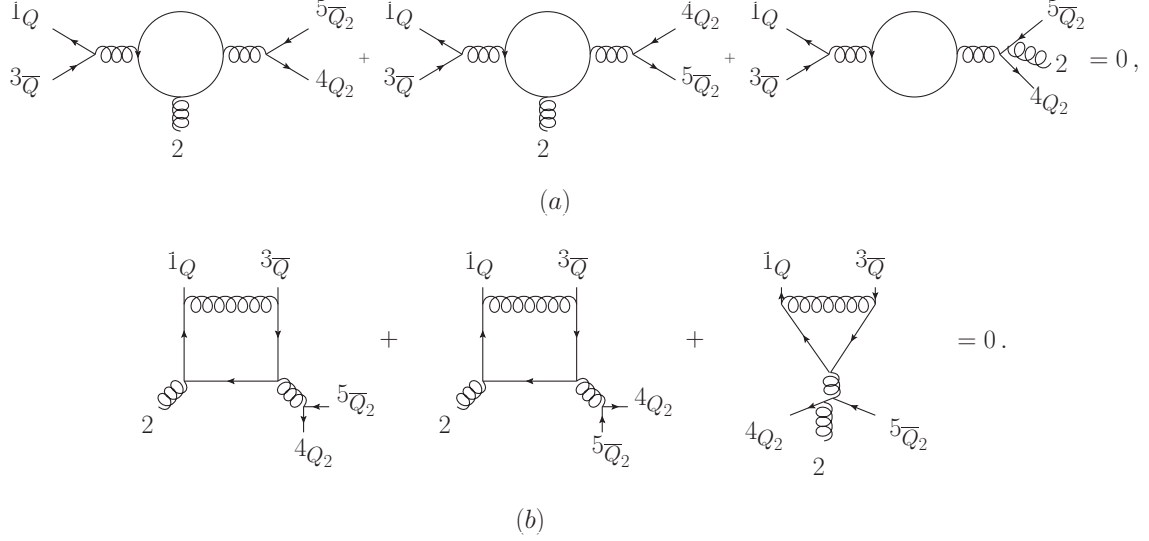


FIG. 3: Parent diagram representation of relations between multi-quark primitive amplitudes: Diagrams (a) show a vanishing sum of primitive amplitudes associated to parent diagrams with a closed fermion loop, as in eq. (3.11). Diagrams (b) show a vanishing sum of primitive amplitudes with at least one gluon in the loop, the pictorial form of eq. (3.12). The relations originate from exchanging the ordering of the fermion pair  $\{4_{Q_2}, 5_{\bar{Q}_2}\}$ , which gives a relative sign. Parent diagrams represent classes of colour-ordered Feynman diagrams. The contributions of all colour-ordered Feynman diagrams cancel once the asymmetry of the fermion-fermion-gluon vertices is taken into account.

with the parent diagrams shown in fig. 3. Similarly, relations may be found for diagrams with no closed internal fermion line,

$$A^{\text{LL}}(1_Q, 3_{\bar{Q}}, 5_{\bar{Q}_2}, 4_{Q_2}, 2) + A^{\text{LR}}(1_Q, 3_{\bar{Q}}, 4_{Q_2}, 5_{\bar{Q}_2}, 2) + A^{\text{LL}}(1_Q, 3_{\bar{Q}}, 5_{\bar{Q}_2}, 2, 4_{Q_2}) = 0, \quad (3.12)$$

with the parent diagrams shown in fig. 3 (b).

For both diagrammatic equations, (a) and (b) in fig. 3, the same mechanism is at work. Contributions from the first two diagrams, respectively, with a direct  $(4_{Q_2}, 5_{\bar{Q}_2}, \text{gluon})$ -vertex cancel against the ones with a direct  $(5_{\bar{Q}_2}, 4_{Q_2}, \text{gluon})$ -vertex, given that the exchange of quarks  $4_{Q_2} \leftrightarrow 5_{\bar{Q}_2}$  introduces a relative minus-sign. The remaining contributions include Feynman diagrams with the gluon moved onto the fermion line. For the first parent diagram in fig. 3 that would be gluon emission from  $4_{Q_2}$ , and for the second parent diagram emission from  $5_{\bar{Q}_2}$ . These contributions are distinct and it is the role of the Feynman diagrams represented by the third parent diagram, to cancel off these remaining pieces.

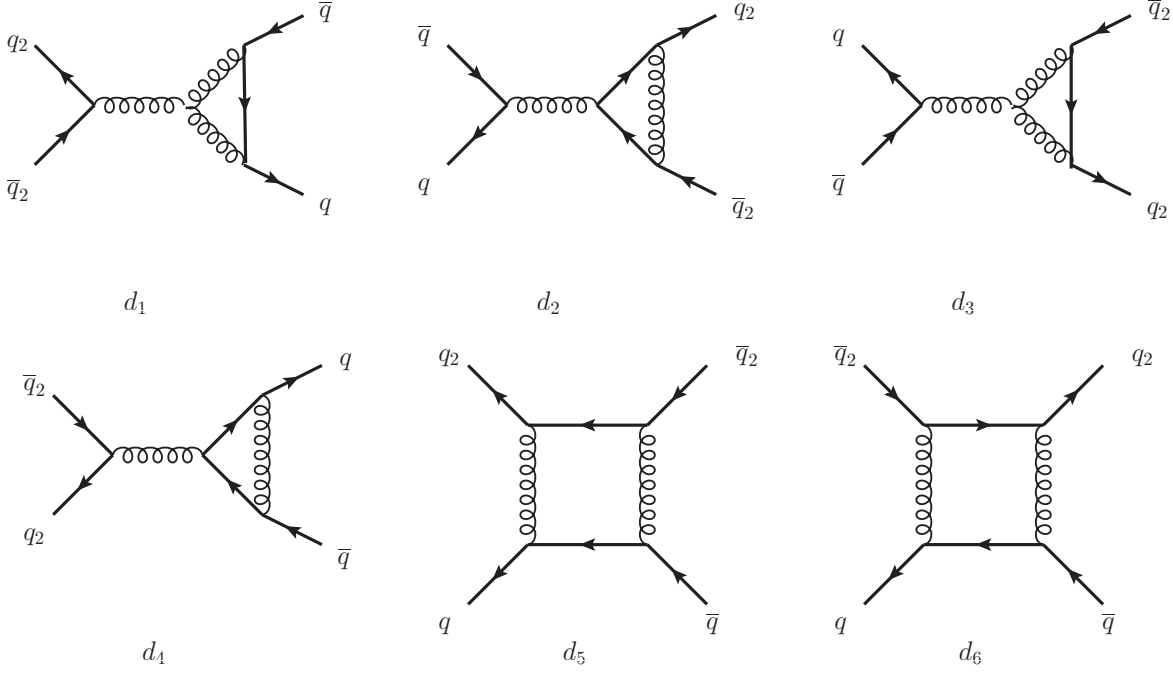


FIG. 4: Feynman diagrams  $d_i$  contributing to the four-quark amplitude. For simplicity we consider only box and triangle diagrams. These are sufficient to obtain the colour decomposition of the four-quark partial amplitudes.

### C. A four-point example

To illustrate the method described in the previous section we present here a fully worked example. We consider the amplitude for scattering of two pairs of different flavour quarks,

$$\mathcal{A}(1_q, 2_{\bar{q}}, 3_{q_2}, 4_{\bar{q}_2}). \quad (3.13)$$

To keep things as simple as possible we will ignore contributions with closed fermion loops, though in our final results these pieces are of course included. We make one further simplification for transparency of the example: we consider six Feynman diagrams ( $N_d = 6$ ), illustrated in figure 4, and drop bubble diagrams. These diagrams are sufficient for the present example. After dressing them with colour (quarks and anti-quarks live in the fundamental and anti-fundamental representations of  $SU(N_c)$  respectively), and simplifying using eq. (2.3), we find two distinct colour structures ( $N_P = 2$ ),

$$C_1 = \delta_{i_1}^{\bar{i}_2} \delta_{i_3}^{\bar{i}_4}, \quad C_2 = \delta_{i_1}^{\bar{i}_4} \delta_{i_3}^{\bar{i}_2}. \quad (3.14)$$



The amplitude is a linear combination of  $C_1$  and  $C_2$ ,

$$\mathcal{A}(1_q, 2_{\bar{q}}, 3_{q_2}, 4_{\bar{q}_2}) = A_1^{\text{partial}}(1_q, 2_{\bar{q}}; 3_{q_2}, 4_{\bar{q}_2}) C_1 + A_2^{\text{partial}}(1_q, 4_{\bar{q}_2}; 3_{q_2}, 2_{\bar{q}}) C_2. \quad (3.15)$$

The expression of the partial amplitudes,  $A_1^{\text{partial}}(1_q, 2_{\bar{q}}; 3_{q_2}, 4_{\bar{q}_2})$  and  $A_2^{\text{partial}}(1_q, 4_{\bar{q}_2}; 3_{q_2}, 2_{\bar{q}})$ , in terms of the Feynman diagrams in figure 4 is described in (3.2) through the  $2 \times 6$  matrix of coefficients  $K_i^j$ ,

$$\{K_i^j\} = \begin{pmatrix} -1 & \frac{1}{N_c^2} & -1 & \frac{1}{N_c^2} & 1 + \frac{1}{N_c^2} & \frac{1}{N_c^2} \\ N_c & -\frac{1}{N_c} & N_c & -\frac{1}{N_c} & -\frac{2}{N_c} & N_c - \frac{2}{N_c} \end{pmatrix}, \quad (3.16)$$

when contracted with the vector of Feynman diagrams  $d_j$ . The top row of this expression relates to  $C_1$ , and the bottom row to  $C_2$ .

To find the primitives, we must dress the amplitude with colour assuming all particles are in the adjoint representation, and then extract the primitives as the coefficients of the single trace structures. We find

$$A^{LL}(1_Q, 2_{\bar{Q}}, 4_{\bar{Q}_2}, 3_{Q_2}) = -d_4, \quad (3.17)$$

$$A^{LL}(1_Q, 3_{Q_2}, 4_{\bar{Q}_2}, 2_{\bar{Q}}) = -d_2, \quad (3.18)$$

$$A^{LL}(1_Q, 4_{\bar{Q}_2}, 3_{Q_2}, 2_{\bar{Q}}) = d_1 + d_3 + d_6, \quad (3.19)$$

$$A^{LR}(1_Q, 2_{\bar{Q}}, 3_{Q_2}, 4_{\bar{Q}_2}) = d_4, \quad (3.20)$$

$$A^{LR}(1_Q, 3_{Q_2}, 4_{\bar{Q}_2}, 2_{\bar{Q}}) = d_5 - d_3 - d_1, \quad (3.21)$$

$$A^{LR}(1_Q, 4_{\bar{Q}_2}, 3_{Q_2}, 2_{\bar{Q}}) = d_2. \quad (3.22)$$

Already at this level we observe that the primitive amplitudes are related as,

$$\begin{aligned} A^{LL}(1_Q, 2_{\bar{Q}}, 4_{\bar{Q}_2}, 3_{Q_2}) &= -A^{LR}(1_Q, 2_{\bar{Q}}, 3_{Q_2}, 4_{\bar{Q}_2}), \\ A^{LL}(1_Q, 3_{Q_2}, 4_{\bar{Q}_2}, 2_{\bar{Q}}) &= -A^{LR}(1_Q, 4_{\bar{Q}_2}, 3_{Q_2}, 2_{\bar{Q}}). \end{aligned} \quad (3.23)$$

These relations are an example of the ones discussed in section IIIB. They are not direct consequences of the symmetry properties of the primitive amplitudes (2.21), (2.22) and (2.23). Rather they are explained by the anti-symmetry of the colour-ordered fermion-fermion-gluon vertex. In eqs. (3.23) the exchange  $3 \leftrightarrow 4$  and  $LL \leftrightarrow LR$  relates the primitives up to a sign. This can also be inferred from the diagrams  $d_2$  and  $d_3$  in fig. 4. Following our earlier notation (3.6) the equations (3.17)-(3.22) are expressed through a matrix of

coefficients  $L_k^j$  and a vector of primitives  $A_k^{D_k}$ ,

$$\{L_k^j\} = \begin{pmatrix} 0 & 0 & 0 & -1 & 0 & 0 \\ 0 & -1 & 0 & 0 & 0 & 0 \\ 1 & 0 & 1 & 0 & 0 & 1 \\ 0 & 0 & 0 & 1 & 0 & 0 \\ -1 & 0 & -1 & 0 & 1 & 0 \\ 0 & 1 & 0 & 0 & 0 & 0 \end{pmatrix}, \quad \{A_k^{D_k}\} = \begin{pmatrix} A^{LL}(1_Q, 2_{\overline{Q}}, 4_{\overline{Q}_2}, 3_{Q_2}) \\ A^{LL}(1_Q, 3_{Q_2}, 4_{\overline{Q}_2}, 2_{\overline{Q}}) \\ A^{LL}(1_Q, 4_{\overline{Q}_2}, 3_{Q_2}, 2_{\overline{Q}}) \\ A^{LR}(1_Q, 2_{\overline{Q}}, 3_{Q_2}, 4_{\overline{Q}_2}) \\ A^{LR}(1_Q, 3_{Q_2}, 4_{\overline{Q}_2}, 2_{\overline{Q}}) \\ A^{LR}(1_Q, 4_{\overline{Q}_2}, 3_{Q_2}, 2_{\overline{Q}}) \end{pmatrix}. \quad (3.24)$$

We note that  $L$  is generally not square, though in this case it is because we chose a reduced number of Feynman diagrams, which happens to be equal to the number of primitive amplitudes.

The solution to equation (3.7) can be found by eliminating the  $d_i$  from eqns. (3.2) using linear combinations of the primitive amplitudes (3.6). We obtain the coefficient matrix  $Z_i^k$  by solving the linear system of equations (3.8) with **Mathematica** [61].

It turns out that there are many different solutions, reflecting the relations (3.23) between primitive amplitudes. This is a new feature for multiple quark line processes that is not observed in the purely gluonic, or single quark line cases. In fact, the matrix  $\{L_k^j\}$  is a  $6 \times 6$  matrix with rank four. The associated null space (3.9) is two-dimensional and given by the two vectors  $(Z_i^{\text{rel}})^k$  with  $i = 1, 2$ . In matrix notation we have,

$$(Z_i^{\text{rel}})^k = \begin{pmatrix} 1 & 0 & 0 & 1 & 0 & 0 \\ 0 & 1 & 0 & 0 & 0 & 1 \end{pmatrix}. \quad (3.25)$$

The null vectors imply the same relations given already in eqs. (3.23).

The solutions are represented as a  $N_P \times N_{\text{prim}} = 2 \times 6$  matrix  $Z$  as follows

$$Z_i^k = \begin{pmatrix} -\frac{1}{N_c^2} + \alpha & -\frac{1}{N_c^2} + \beta & \frac{1}{N_c^2} & \alpha & 1 + \frac{1}{N_c^2} & \beta \\ \frac{1}{N_c} + \gamma & \frac{1}{N_c} + \delta & N_c - \frac{2}{N_c} & \gamma & -\frac{2}{N_c} & \delta \end{pmatrix}, \quad (3.26)$$

where  $\alpha, \beta, \gamma$  and  $\delta$  are arbitrary complex numbers parameterising the solution space. The first row of  $Z$  gives the six coefficients of the primitive amplitudes, in the basis (3.17), needed to construct the coefficient of the colour structure  $C_1$ . The second row does the same thing for the structure  $C_2$ .

Anticipating the explicit results in section IV we relate the solutions (3.26) to the attached data-files. Compared to the explicit colour decompositions given in the attached file

(partials\_4q.dat) we have the following choices for the parameters,  $\alpha = 0$ ,  $\beta = \frac{1}{N_c^2}$ ,  $\gamma = 0$ , and  $\delta = -\frac{1}{N_c}$ . In this way we avoid the use of two out of six primitive amplitudes.

## IV. RESULTS

General expressions for the decomposition of partial amplitudes in terms of sets of primitive amplitudes are available in the literature for two classes of process, the  $n$ -gluon [16, 17] and the two-quark  $n$ -gluon [18] QCD amplitudes. A fixed-multiplicity decomposition of four-quark amplitudes was given in [19, 46] and for an additional gluon in [47]. In fact these expressions were first given including particles neutral under the gauge group. Here we generate sets of partial amplitudes algorithmically for a given scattering process with emphasis on the cases of six- and seven-parton QCD amplitudes including four quarks and six quarks. The generalisation of these to amplitudes including a single colourless vector-boson is straightforward, and will be discussed in section IV C. In the recent results [11, 12] for  $V$ -boson plus four-jet NLO cross sections, a leading-colour approximation was used in the virtual contribution. In the following we will present a corresponding full-colour distribution.

### A. New colour decompositions for QCD amplitudes

We present first our results for partial amplitudes in terms of primitive amplitudes with six and seven coloured partons. We focus entirely on processes with distinct quark flavours. This incurs no loss of generality, because all other cases can be derived as simple linear combinations of these.

As an example we show in fig. 5 one of the partial amplitudes relevant for six-quark processes. In this case there are 26 contributing primitives, each with its own  $N_c$ -dependent coefficient. There are three turner labels, one for each quark line. As described in section III, when there are multiple quark lines present the expressions are not unique, as the primitive amplitudes satisfy a set of relations.

It is interesting to consider in comparison the leading-colour part of the above partial amplitude, as shown in fig. 6. Formally, the leading colour part of the partial amplitude is here defined as the leading terms in the limit  $N_c \gg 1$  and  $n_f \gg 1$  with the ratio  $N_c/n_f$  fixed. The number of contributing primitive amplitudes is strongly reduced when subleading in

```

* Partial: { q(1) qb2(2) , q2(3) qb3(4) , q3(5) qb(6) }

born { Q(1) Qb2(2) Q2(3) Qb3(4) Q3(5) Qb(6) | 1 }
loop {
  LLL | Q(1) Qb2(2) Q2(3) Qb3(4) Q3(5) Qb(6) | -3/Nc + Nc
  LLR | Q(1) Qb2(2) Q2(3) Q3(5) Qb3(4) Qb(6) | -2/Nc
  LRL | Q(1) Q2(3) Qb2(2) Qb3(4) Q3(5) Qb(6) | -2/Nc
  LRR | Q(1) Q2(3) Qb2(2) Q3(5) Qb3(4) Qb(6) | -1/Nc
  LRL | Q(1) Qb3(4) Q3(5) Q2(3) Qb2(2) Qb(6) | -1/Nc
  LLR | Q(1) Q3(5) Qb3(4) Qb2(2) Q2(3) Qb(6) | -1/Nc
  LRR | Q(1) Q3(5) Qb3(4) Q2(3) Qb2(2) Qb(6) | -2/Nc
  LLL | Q(1) Qb2(2) Qb3(4) Q3(5) Q2(3) Qb(6) | 1/Nc
  LRL | Q(1) Qb2(2) Qb3(4) Q3(5) Q2(3) Qb(6) | -1/Nc
  LRR | Q(1) Qb2(2) Q3(5) Qb3(4) Q2(3) Qb(6) | -1/Nc
  LRL | Q(1) Q2(3) Qb3(4) Q3(5) Qb2(2) Qb(6) | -1/Nc
  LLL | Q(1) Qb3(4) Qb2(2) Q2(3) Q3(5) Qb(6) | 1/Nc
  LLR | Q(1) Qb3(4) Qb2(2) Q2(3) Q3(5) Qb(6) | -1/Nc
  LRR | Q(1) Qb3(4) Q2(3) Qb2(2) Q3(5) Qb(6) | -1/Nc
  LLR | Q(1) Q3(5) Qb2(2) Q2(3) Qb3(4) Qb(6) | -1/Nc
  LLL | Q(1) Qb3(4) Q3(5) Qb(6) Qb2(2) Q2(3) | 1/Nc
  LLR | Q(1) Q3(5) Qb3(4) Qb(6) Qb2(2) Q2(3) | 1/Nc
  LLL | Q(1) Qb2(2) Q2(3) Qb(6) Qb3(4) Q3(5) | 1/Nc
  LRL | Q(1) Q2(3) Qb2(2) Qb(6) Qb3(4) Q3(5) | 1/Nc
  LLR | Q(1) Qb2(2) Q2(3) Qb3(4) Q3(5) Qb(6) | -1/Nc
  LRL | Q(1) Qb2(2) Q2(3) Qb3(4) Q3(5) Qb(6) | -1/Nc
  LLL | Q(1) Qb(6) Qb2(2) Q2(3) Qb3(4) Q3(5) | 2/Nc
  LLR | Q(1) Qb(6) Qb2(2) Q2(3) Q3(5) Qb3(4) | 1/Nc
  LRL | Q(1) Qb(6) Q2(3) Qb2(2) Qb3(4) Q3(5) | 1/Nc
  LLL | Q(1) Qb(6) Qb3(4) Q3(5) Qb2(2) Q2(3) | -1/Nc
  nfLLL | Q(1) Qb2(2) Q2(3) Qb3(4) Q3(5) Qb(6) | nf
}

```

FIG. 5: A six-quark partial amplitude given as a decomposition into primitive amplitudes. The shown partial amplitude is an extract from the file `partials_6q.dat` in the ancillary material [56].

```

* Partial: { q(1) qb2(2) , q2(3) qb3(4) , q3(5) qb(6) }

born { Q(1) Qb2(2) Q2(3) Qb3(4) Q3(5) Qb(6) | 1 }
loop {
  LLL | Q(1) Qb2(2) Q2(3) Qb3(4) Q3(5) Qb(6) | Nc
  nfLLL | Q(1) Qb2(2) Q2(3) Qb3(4) Q3(5) Qb(6) | nf
}

```

FIG. 6: Leading colour six-quark partial amplitude given as a decomposition into primitive amplitudes.

$N_c$  contributions are removed. This is one of the reasons for using this approximation when constructing NLO partonic Monte Carlo programs — the leading-colour amplitude can be numerically evaluated much faster.

The leading-colour contribution to the decomposition of quark amplitudes is easily ob-

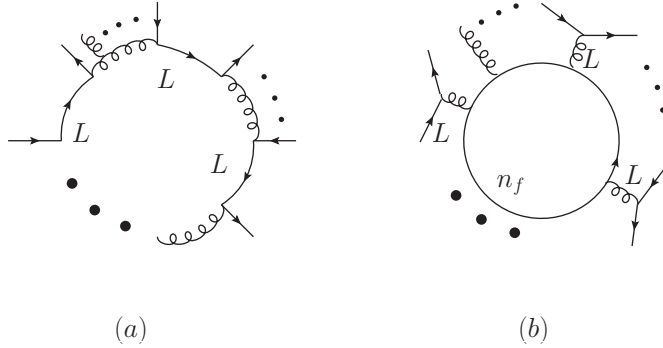


FIG. 7: Generic leading-colour parent diagrams for the leading partial amplitudes: (a) a  $(LL \cdots L)$ -turner and (b) a  $(n_f LL \cdots L)$ -turner. External gluons may be added if directly emitted from the gluonic loop propagators in (a) or from the fermion loop in (b).

tained for arbitrary multiplicities following a few simple rules: 1) partial amplitudes with vanishing or subleading (in  $1/N_c$ ) tree-level contributions are set to zero. 2) the particle orderings of the leading-colour primitive amplitudes follow that of the born amplitude. 3) Two particular types of left-right-turner labels are singled out leading to the two types of parent diagrams as shown in fig. 7. In (a) we show the primitive amplitude with multiple left-turner quark lines including gluon propagators in the loop. It is denoted by the label  $(LLL \cdots)$ . The associated parent diagram has both gluon and fermion propagators. The number of propagators matches the multiplicity of the amplitude, here meant to be  $n$ . The second primitive amplitude, (b), has a closed fermion loop with each fermion line coupled to it via gluons. The label specifying the fermion routing is then  $(n_f LLL \cdots)$ . The associated parent diagram has only fermion propagators. The general structure is manifest in the two-, four- and six-quark cases discussed here.

## B. Explicit results in attached text files

The expressions for the partial amplitudes can be found in the location [56] in the respective text files

$$\text{partials\_n}_g \text{ g n}_q \text{ q.dat} \quad (4.1)$$

provided for all independent partial amplitudes with  $n_g$  gluons and  $n_q$  quarks. The format of the files has been described in section II E. We give the cases,

$$\{(n_g, n_q)\} = \{(0, 4), (1, 4), (2, 4), (3, 4), (0, 6), (1, 6)\}. \quad (4.2)$$

Together with the  $(n, 0)$  and  $(n - 2, 2)$  assemblies given in refs. [17, 18], this completes the colour decomposition of QCD amplitudes up to and including seven colour-charged external states.

We confirmed that two independent implementations of the algorithm described in this paper produce identical numerical results for partial amplitudes. The explicit expressions from each implementation match up to application of the relations described in section III B. Furthermore, the expressions for the partial amplitudes are checked against the existing results in the literature where available. In particular, for all new six-parton and seven-parton expressions we confirmed numerically that the virtual squared matrix elements give the expected pole structure [62] for single and double poles in the dimensional regularization parameter  $\epsilon$ . We used BLACKHAT [31] and SHERPA [63] for this numerical check. A further numerical check is provided by the recent public release of HELAC-1LOOP [42, 64], which we have used to check all our 6-parton results.

In addition to the expressions for pure QCD amplitudes, the attached files (for the download location see [56])

$$\text{partials\_n\_g n\_q 2l.dat} \quad (4.3)$$

give their generalisation to include a colour neutral lepton pair. These contributions are the ones relevant for the computation of  $W + 4\text{-jet}$  production, as we discuss in the next section.

### C. Application to $W + 4\text{ jets}$

The results we have presented are crucial for the application of the colour-ordered approach to vector-boson production in association with multiple jets at NLO. With the colour decomposition of the pure QCD amplitudes one can obtain rather simply their generalisations to include colourless states. We discuss here how to obtain the colour decomposition of  $W + \text{jets}$  amplitudes, and give a comparison of leading-colour versus full-colour differential distributions of the virtual part of  $W + 4\text{-jet}$  production at the LHC.

### 1. *Inserting colour-less states.*

Amplitudes with additional colourless objects – leptons, vector bosons, Higgs bosons, etc. – can be accommodated in the decomposition of partial amplitudes into primitive amplitudes starting from the pure QCD decomposition.

For  $W + n$ -jet production we consider the decay of the  $W$ -boson into a lepton pair,  $\nu_\ell$  and  $\ell$ . These amplitudes can be obtained by first computing amplitudes with a virtual photon that is emitted from a quark  $q$  and decays to a charged lepton pair  $(\ell_L, \ell_R)$ . In a second step, the conversion to a lepton and a neutrino  $(\nu_{\ell L}, \ell_R)$  is done by multiplicative factors including couplings and  $W$ -boson propagator terms. Details about this conversion are explained in refs. [19, 65]. With this approach we consider amplitudes with a lepton pair coupled to a quark pair via an off-shell photon. In fact, we do not need to consider all such amplitudes; we can drop the emission of the photon from an internal quark loop as these kind of emissions are forbidden for  $W$ -production due to flavour non-conservation.

With the basic understanding that the lepton pair is coupled to the quark with flavour one, it is straightforward to transcribe the pure QCD partial amplitude into the one including a virtual photon decayed into a lepton pair, as displayed in fig. 8. The full scattering matrix elements can be built from these basic amplitudes [19].

### 2. *Full colour differential distributions.*

The transverse momentum,  $p_T$ , of the accompanying jets is one of the most important observables in  $W$ -boson production. For  $W + 4$ -jet production at NLO the differential  $p_T$  distributions of the leading four jets have been given in [11]. In that paper a leading-colour approximation was used for the virtual parts<sup>3</sup>. Here we compute for the first time the subleading-colour corrections and compare the size of leading-colour and full-colour virtual contributions. We use the same basic setup and cuts as in [11]. The virtual contributions are computed using on-shell methods via the BLACKHAT package, while SHERPA is used to perform the phase-space integration. The combination of these two programs has been used extensively for studying hadron collider phenomenology at NLO [3, 5, 6, 11, 12, 31, 66, 67], and is very well tested. For simplicity we will here focus on the  $p_T$  distribution of the fourth

---

<sup>3</sup> The other parts - the born and real emission - were evaluated without any colour-based approximation.

```

* Partial: { q(1) qb2(2) , q2(3) qb3(4) , q3(5) qb(6) ; l(7) lb(8) }

born { Q(1) Qb2(2) Q2(3) Qb3(4) Q3(5) Qb(6) l(7) lb(8) | 1 }
loop {
  LLL | Q(1) Qb2(2) Q2(3) Qb3(4) Q3(5) Qb(6) l(7) lb(8) | -3/Nc + Nc
  LLR | Q(1) Qb2(2) Q2(3) Q3(5) Qb3(4) Qb(6) l(7) lb(8) | -2/Nc
  LRL | Q(1) Q2(3) Qb2(2) Qb3(4) Q3(5) Qb(6) l(7) lb(8) | -2/Nc
  LRR | Q(1) Q2(3) Qb2(2) Q3(5) Qb3(4) Qb(6) l(7) lb(8) | -1/Nc
  LRL | Q(1) Qb3(4) Q3(5) Q2(3) Qb2(2) Qb(6) l(7) lb(8) | -1/Nc
  LLR | Q(1) Q3(5) Qb3(4) Qb2(2) Q2(3) Qb(6) l(7) lb(8) | -1/Nc
  LRR | Q(1) Q3(5) Qb3(4) Q2(3) Qb2(2) Qb(6) l(7) lb(8) | -2/Nc
  LLL | Q(1) Qb2(2) Qb3(4) Q3(5) Q2(3) Qb(6) l(7) lb(8) | 1/Nc
  LRL | Q(1) Qb2(2) Qb3(4) Q3(5) Q2(3) Qb(6) l(7) lb(8) | -1/Nc
  LRR | Q(1) Qb2(2) Q3(5) Qb3(4) Q2(3) Qb(6) l(7) lb(8) | -1/Nc
  LRL | Q(1) Q2(3) Qb3(4) Q3(5) Qb2(2) Qb(6) l(7) lb(8) | -1/Nc
  LLL | Q(1) Qb3(4) Qb2(2) Q2(3) Q3(5) Qb(6) l(7) lb(8) | 1/Nc
  LLR | Q(1) Qb3(4) Qb2(2) Q2(3) Q3(5) Qb(6) l(7) lb(8) | -1/Nc
  LRR | Q(1) Qb3(4) Q2(3) Qb2(2) Q3(5) Qb(6) l(7) lb(8) | -1/Nc
  LLR | Q(1) Q3(5) Qb2(2) Q2(3) Qb3(4) Qb(6) l(7) lb(8) | -1/Nc
  LLL | Q(1) Qb3(4) Q3(5) Qb(6) Qb2(2) Q2(3) l(7) lb(8) | 1/Nc
  LLR | Q(1) Q3(5) Qb3(4) Qb(6) Qb2(2) Q2(3) l(7) lb(8) | 1/Nc
  LLL | Q(1) Qb2(2) Q2(3) Qb(6) Qb3(4) Q3(5) l(7) lb(8) | 1/Nc
  LRL | Q(1) Q2(3) Qb2(2) Qb(6) Qb3(4) Q3(5) l(7) lb(8) | 1/Nc
  LLR | Q(1) Qb2(2) Q2(3) Qb3(4) Q3(5) Qb(6) l(7) lb(8) | -1/Nc
  LRL | Q(1) Qb2(2) Q2(3) Qb3(4) Q3(5) Qb(6) l(7) lb(8) | -1/Nc
  LLL | Q(1) Qb(6) Qb2(2) Q2(3) Qb3(4) Q3(5) l(7) lb(8) | 2/Nc
  LLR | Q(1) Qb(6) Qb2(2) Q2(3) Q3(5) Qb3(4) l(7) lb(8) | 1/Nc
  LRL | Q(1) Qb(6) Q2(3) Qb2(2) Qb3(4) Q3(5) l(7) lb(8) | 1/Nc
  LLL | Q(1) Qb(6) Qb3(4) Q3(5) Qb2(2) Q2(3) l(7) lb(8) | -1/Nc
  nfLLL | Q(1) Qb2(2) Q2(3) Qb3(4) Q3(5) Qb(6) l(7) lb(8) | nf
}

```

FIG. 8: Six-quark two-lepton partial amplitude given as a decomposition into primitive amplitudes.

The leptons couple via virtual photon exchange to the quarks with flavour one,  $Q$  and  $\bar{Q}$ . These partial amplitudes are building blocks of the scattering amplitudes for  $W$ -boson production.

jet.

The leading-colour approximation used here differs from the one in ref. [11] by terms subleading in  $1/N_c$ . Both approximations drop only finite terms (in the  $1/\epsilon$  expansion) and retain the full colour dependence of the IR-divergent pieces. Our explicit setup for the finite parts is given in the following. Initially, our virtual contributions are computed in the four-dimensional helicity (FDH) scheme [68, 69], which is most convenient for the use of helicity amplitudes. Only in the end are the virtual amplitudes converted to the more standard 't Hooft-Veltman scheme [70] used as input for SHERPA. This conversion is done through a simple shift proportional to the born matrix element (see e.g. section six in [19]). Our leading-colour approximation contains the full scheme shift contributions, including terms



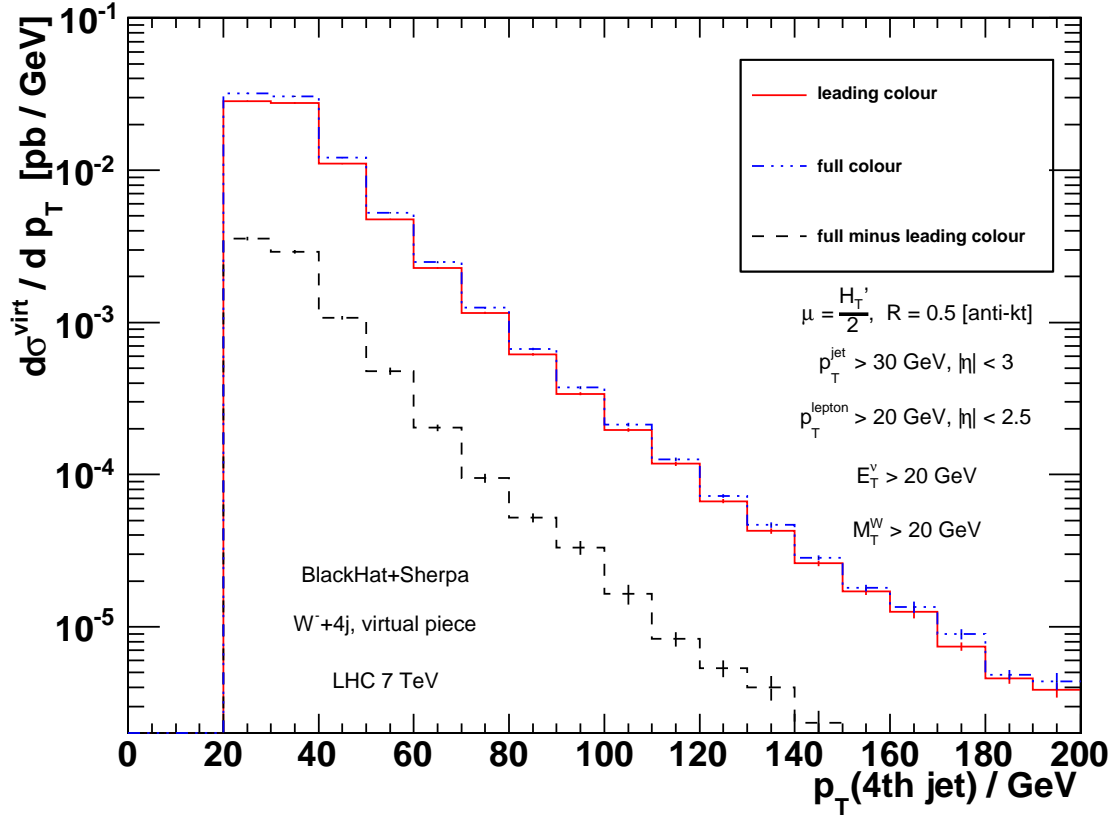


FIG. 9: A comparison of the full and leading-colour virtual contributions to the  $p_T$  distribution of the fourth jet in  $W^-+4\text{-jet}$  production at the 7 TeV LHC. Their difference (full-minus-leading-colour) is also shown. We show not a physical cross section, but rather a particular piece of it. The subleading-colour contribution is suppressed by a factor of  $1/N_c^2$ , approximately uniformly. The vertical lines in the center of each bin, indicate integration errors.

subleading in  $1/N_c$ . In both approaches, the partial amplitudes include the leading terms in the formal limit  $N_c \gg 1$  and  $n_f \gg 1$  with  $N_c/n_f$  fixed. Here, all interference terms of the non-zero partial amplitudes are kept. To point out one difference to ref. [11], there, in a more conventional approach, only the leading-colour interference terms were kept.

The comparison of the full-colour and leading-colour virtual contributions to the  $p_T$  distribution of the fourth jet in  $W^-+4\text{-jet}$  production at the LHC is shown in fig. 9. Also displayed are the subleading-colour contributions by themselves, labelled as “full-minus-leading-colour”. In order to obtain the full parton level differential cross-section one must

add the real and born contributions in the usual way. The complete  $p_T$  distribution, including born, real and leading-colour virtual contributions, has been given already in [11].

We confirm that the subleading-colour contribution is suppressed uniformly over the  $p_T$  range from 20 GeV to 200 GeV. The suppression appears consistent with the expected factor of  $1/N_c^2$  with  $N_c = 3$ . With the leading-colour virtual part accounting for about 20% of the leading-colour total cross section, as already observed in refs. [5, 11], the subleading-colour virtual part amounts to less than a 3% correction. Although numerically similar, the present leading colour approximation and the one from ref. [11] are not identical. We have checked that our conclusions hold for both definitions, namely that sub-leading colour contributions are at the level of a few percent.

A possible exception to the uniform suppression are zeros of the leading-colour virtual cross section. Such zeros are not excluded on general grounds, as the virtual piece alone is not physical. A priori, there is no reason to assume that the vanishing of the leading-colour contribution forces also the vanishing of the subleading-colour contribution. Close to a zero of the leading-colour contribution we naturally expect a relative enhancement of the subleading-colour piece. In the range of the distribution presented in fig. 9 we do not observe such behaviour and observe a uniform suppression of the subleading-colour contribution. We leave a more thorough consideration of this issue, as well as a more detailed phenomenological analysis, to future work.

## V. CONCLUSION

Recent years have seen impressive progress in NLO parton level computations relevant for LHC physics. In particular, the unitarity and on-shell approaches have opened new possibilities for the computation of one-loop scattering amplitudes.

An important ingredient in these advances is a clear theoretical understanding of the amplitudes, which enables an efficient structuring of the calculation. This progress has made possible high multiplicity parton-level predictions at NLO for generic physics processes and models. The colour organisation discussed here is one important aspect towards automation in the colour-ordered approach.

We have presented explicit expressions for the colour decomposition of pure-QCD amplitudes with up to seven partons. We also gave their extension to include a leptonically

decaying  $W$ -boson. Whereas leading-colour expressions are simple to write down, terms subleading in  $1/N_c$  are not easily obtained. We have described a general algorithm for obtaining such subleading terms, applicable to cases with any number of fermion pairs.

Although we give explicit expressions, typically these are not unique. There exist relations between primitive amplitudes which originate in the anti-symmetry of the fermion-fermion-gluon colour-ordered three-point vertex. We expect that these “fermion-flip” relations will be important in obtaining all- $n$  formulae for multi-quark amplitudes, as exist already for the pure-gluon [17] and two-quark [18] cases (see also [60]).

Contributions to the virtual corrections at subleading order in  $1/N_c$  have been shown to be uniformly small over phase space for  $W + 1, 2, 3$ -jet production in [5]. However, no general theorems are available to assess the size of subleading-colour terms in all regions of phase space *a priori*. We have applied our new results to understand the effect of subleading-colour virtual contributions to distributions of  $W + 4$ -jet production. We showed that for the fourth-jet  $p_T$  distribution the effect is small (a few percent) and observe a similar behaviour for other distributions. A detailed study of the physics, including subleading-colour contributions, to pure jets and vector-boson plus jets could be carried out in the future using the results of this article.

In summary, we have presented a general method towards a colour-ordered approach for loop computations with many coloured final states. We expect these results will aid in physics studies of relevance to the LHC in the near future.

## Acknowledgments

We would like to thank Zvi Bern, Giovanni Diana, Lance Dixon, Fernando Febres Cordero, Stefan Höche, David Kosower and Daniel Maître for many useful discussions and comments on the manuscript. HI would like to thank the School of Physics and Astronomy at Tel-Aviv University for their hospitality during the completion of this work.

This research was supported by the US Department of Energy under contracts DE-FG03-91ER40662. HI’s work is supported by a grant from the US LHC Theory Initiative through

- [1] J. R. Andersen *et al.* [ SM and NLO Multileg Working Group Collaboration ], [arXiv:1003.1241 [hep-ph]].
- [2] Z. Nagy, Phys. Rev. Lett. **88**, 122003 (2002). [arXiv:hep-ph/0110315 [hep-ph]]; Z. Nagy, Phys. Rev. **D68**, 094002 (2003). [hep-ph/0307268].
- [3] C. F. Berger *et al.*, Phys. Rev. Lett. **102**, 222001 (2009) [0902.2760 [hep-ph]].
- [4] R. K. Ellis, K. Melnikov and G. Zanderighi, Phys. Rev. D **80**, 094002 (2009) [0906.1445 [hep-ph]].
- [5] C. F. Berger *et al.*, Phys. Rev. D **80**, 074036 (2009) [0907.1984 [hep-ph]].
- [6] C. F. Berger *et al.*, Phys. Rev. D **82**, 074002 (2010) [1004.1659 [hep-ph]].
- [7] A. Bredenstein, A. Denner, S. Dittmaier and S. Pozzorini, JHEP **0808**, 108 (2008) [0807.1248 [hep-ph]]; Phys. Rev. Lett. **103**, 012002 (2009) [0905.0110 [hep-ph]].
- [8] K. Melnikov, M. Schulze, Nucl. Phys. **B840**, 129-159 (2010). [arXiv:1004.3284 [hep-ph]];
- [9] T. Binoth, N. Greiner, A. Guffanti, J. P. Guillet, T. Reiter and J. Reuter, Phys. Lett. B **685**, 293 (2010) [0910.4379 [hep-ph]];
- [10] G. Bevilacqua, M. Czakon, C. G. Papadopoulos, R. Pittau and M. Worek, JHEP **0909**, 109 (2009) [0907.4723 [hep-ph]]; G. Bevilacqua, M. Czakon, C. G. Papadopoulos and M. Worek, Phys. Rev. Lett. **104**, 162002 (2010) [1002.4009 [hep-ph]]; G. Bevilacqua, M. Czakon, A. van Hameren, C. G. Papadopoulos, M. Worek, JHEP **1102**, 083 (2011). [arXiv:1012.4230 [hep-ph]].
- [11] C. F. Berger, Z. Bern, L. J. Dixon, F. Febres Cordero, D. Forde, T. Gleisberg, H. Ita, D. A. Kosower and D. Maître, Phys. Rev. Lett. **106**, 092001 (2011) [arXiv:1009.2338 [hep-ph]].
- [12] H. Ita, Z. Bern, L. J. Dixon, F. F. Cordero, D. A. Kosower, D. Maitre, [arXiv:1108.2229 [hep-ph]].
- [13] G. Bevilacqua, M. Czakon, C. G. Papadopoulos, M. Worek, [arXiv:1108.2851 [hep-ph]].
- [14] F. A. Berends, W. Giele, Nucl. Phys. **B294** (1987) 700.
- [15] M. L. Mangano, Nucl. Phys. **B309**, 461 (1988).
- [16] Z. Bern and D. A. Kosower, Nucl. Phys. B **362**, 389 (1991).
- [17] Z. Bern, L. J. Dixon, D. C. Dunbar and D. A. Kosower, Nucl. Phys. B **425**, 217 (1994)

- [arXiv:hep-ph/9403226].
- [18] Z. Bern, L. J. Dixon and D. A. Kosower, Nucl. Phys. B **437**, 259 (1995) [hep-ph/9409393].
  - [19] Z. Bern, L. J. Dixon and D. A. Kosower, Nucl. Phys. B **513**, 3 (1998) [hep-ph/9708239].
  - [20] C. Duhr, S. Hoeche, F. Maltoni, JHEP **0608**, 062 (2006) [hep-ph/0607057].
  - [21] F. A. Berends, W. T. Giele, Nucl. Phys. **B313**, 595 (1989).
  - [22] F. Caravaglios, M. Moretti, Phys. Lett. **B358**, 332-338 (1995) [hep-ph/9507237]; F. Caravaglios, M. L. Mangano, M. Moretti, R. Pittau, Nucl. Phys. **B539**, 215-232 (1999) [hep-ph/9807570].
  - [23] A. Kanaki, C. G. Papadopoulos, Comput. Phys. Commun. **132**, 306-315 (2000) [hep-ph/0002082]; A. Cafarella, C. G. Papadopoulos, M. Worek, Comput. Phys. Commun. **180**, 1941-1955 (2009) [arXiv:0710.2427 [hep-ph]].
  - [24] M. Moretti, T. Ohl, J. Reuter, In \*2nd ECFA/DESY Study 1998-2001\* 1981-2009 [hep-ph/0102195]; W. Kilian, T. Ohl, J. Reuter, Eur. Phys. J. **C71**, 1742 (2011) [arXiv:0708.4233 [hep-ph]].
  - [25] T. Gleisberg, S. Hoeche, JHEP **0812**, 039 (2008) [arXiv:0808.3674 [hep-ph]].
  - [26] L. J. Dixon and A. Signer, Phys. Rev. D **56**, 4031 (1997) [arXiv:hep-ph/9706285].
  - [27] Z. Bern, L. J. Dixon, D. C. Dunbar and D. A. Kosower, Nucl. Phys. B **435**, 59 (1995) [hep-ph/9409265].
  - [28] Z. Bern and A. G. Morgan, Nucl. Phys. B **467**, 479 (1996) [hep-ph/9511336]; Z. Bern, L. J. Dixon, D. C. Dunbar and D. A. Kosower, Phys. Lett. B **394**, 105 (1997) [hep-th/9611127].
  - [29] Z. Bern, L. J. Dixon and D. A. Kosower, Phys. Rev. D **71**, 105013 (2005) [hep-th/0501240]; Phys. Rev. D **72**, 125003 (2005) [hep-ph/0505055]; Phys. Rev. D **73**, 065013 (2006) [hep-ph/0507005];
  - [30] Z. Bern, N. E. J. Bjerrum-Bohr, D. C. Dunbar and H. Ita, JHEP **0511**, 027 (2005) [arXiv:hep-ph/0507019].
  - [31] C. F. Berger, Z. Bern, L. J. Dixon, F. Febres Cordero, D. Forde, H. Ita, D. A. Kosower and D. Maître, Phys. Rev. D **78**, 036003 (2008) [0803.4180 [hep-ph]].
  - [32] R. Britto, F. Cachazo and B. Feng, Nucl. Phys. B **725**, 275 (2005) [hep-th/0412103].
  - [33] D. Forde, Phys. Rev. **D75**, 125019 (2007). [arXiv:0704.1835 [hep-ph]].
  - [34] G. Ossola, C. G. Papadopoulos and R. Pittau, Nucl. Phys. B **763**, 147 (2007) [hep-ph/0609007]; F. del Aguila, R. Pittau, JHEP **0407**, 017 (2004). [hep-ph/0404120].

- [35] R. K. Ellis, W. T. Giele and Z. Kunszt, JHEP **0803**, 003 (2008) [0708.2398 [hep-ph]].
- [36] W. T. Giele, Z. Kunszt and K. Melnikov, JHEP **0804**, 049 (2008) [0801.2237 [hep-ph]].
- [37] W. T. Giele and G. Zanderighi, JHEP **0806** (2008) 038 [arXiv:0805.2152 [hep-ph]].
- [38] A. Lazopoulos, 0812.2998 [hep-ph];
- [39] J. C. Winter and W. T. Giele, 0902.0094 [hep-ph]; W. Giele, Z. Kunszt, J. Winter, Nucl. Phys. **B840**, 214-270 (2010). [arXiv:0911.1962 [hep-ph]].
- [40] P. Mastrolia, G. Ossola, T. Reiter, F. Tramontano, JHEP **1008**, 080 (2010). [arXiv:1006.0710 [hep-ph]].
- [41] V. Hirschi, R. Frederix, S. Frixione, M. V. Garzelli, F. Maltoni, R. Pittau, JHEP **1105**, 044 (2011) [arXiv:1103.0621 [hep-ph]].
- [42] G. Bevilacqua, M. Czakon, M. V. Garzelli, A. van Hameren, A. Kardos, C. G. Papadopoulos, R. Pittau, M. Worek, [arXiv:1110.1499 [hep-ph]].
- [43] S. Badger, B. Biedermann, P. Uwer, [arXiv:1011.2900 [hep-ph]].
- [44] A. Bredenstein, A. Denner, S. Dittmaier, S. Pozzorini, JHEP **1003**, 021 (2010) [arXiv:1001.4006 [hep-ph]].
- [45] Z. Kunszt, A. Signer, Z. Trocsanyi, Nucl. Phys. **B411**, 397-442 (1994) [hep-ph/9305239]; Z. Kunszt, A. Signer, Z. Trocsanyi, Phys. Lett. **B336**, 529-536 (1994). [hep-ph/9405386].
- [46] Z. Bern, L. J. Dixon, D. A. Kosower, S. Weinzierl, Nucl. Phys. **B489** (1997) 3-23. [hep-ph/9610370].
- [47] R. K. Ellis, W. T. Giele, Z. Kunszt, K. Melnikov, G. Zanderighi, JHEP **0901**, 012 (2009). [arXiv:0810.2762 [hep-ph]].
- [48] M. L. Mangano and S. J. Parke, Phys. Rept. **200**, 301 (1991); L. J. Dixon, in *QCD & Beyond: Proceedings of TASI '95*, ed. D. E. Soper (World Scientific, 1996) [hep-ph/9601359].
- [49] Z. Bern, L. J. Dixon and D. A. Kosower, Ann. Rev. Nucl. Part. Sci. **46**, 109 (1996) [hep-ph/9602280].
- [50] R. K. Ellis, Z. Kunszt, K. Melnikov, G. Zanderighi, [arXiv:1105.4319 [hep-ph]].
- [51] P. Cvitanovic, P. G. Lauwers, P. N. Scharbach, Nucl. Phys. **B186**, 165 (1981).
- [52] M. L. Mangano, S. J. Parke, Z. Xu, Nucl. Phys. **B298** (1988) 653.
- [53] F. A. Berends and W. T. Giele, Nucl. Phys. B **306**, 759 (1988).
- [54] D. A. Kosower, Nucl. Phys. **B315**, 391 (1989).
- [55] W. T. Giele, E. W. N. Glover, Phys. Rev. **D46**, 1980-2010 (1992).

- [56] `anc/partial*_*.dat` in the source of the arXiv version of this manuscript or viewed directly following the instructions at [http://arxiv.org/help/ancillary\\_files](http://arxiv.org/help/ancillary_files).
- [57] P. Nogueira, J. Comput. Phys. **105**, 279-289 (1993).
- [58] J. A. M. Vermaseren, [math-ph/0010025].
- [59] R. Kleiss and H. Kuijf, Nucl. Phys. B **312**, 616 (1989).
- [60] V. Del Duca, L. J. Dixon, F. Maltoni, Nucl. Phys. **B571**, 51-70 (2000). [hep-ph/9910563].
- [61] Wolfram Research, Inc., Mathematica, Version 6.0, Champaign, IL (2007).
- [62] S. Catani, Phys. Lett. **B427** (1998) 161-171. [hep-ph/9802439].
- [63] T. Gleisberg, S. Hoeche, F. Krauss, M. Schonherr, S. Schumann, F. Siegert, J. Winter, JHEP **0902**, 007 (2009). [arXiv:0811.4622 [hep-ph]]. F. Krauss, R. Kuhn, G. Soff, JHEP **0202**, 044 (2002). [hep-ph/0109036]. T. Gleisberg, F. Krauss, Eur. Phys. J. **C53**, 501-523 (2008). [arXiv:0709.2881 [hep-ph]].
- [64] A. van Hameren, C. G. Papadopoulos, R. Pittau, JHEP **0909** (2009) 106 [arXiv:0903.4665 [hep-ph]].
- [65] L. J. Dixon, J. M. Henn, J. Plefka, T. Schuster, JHEP **1101**, 035 (2011). [arXiv:1010.3991 [hep-ph]].
- [66] Z. Bern, G. Diana, L. J. Dixon, F. Febres Cordero, D. Forde, T. Gleisberg, S. Hoeche, H. Ita, D. A. Kosower, D. Maitre, K.J. Ozeren, Phys. Rev. **D84**, 034008 (2011). [arXiv:1103.5445 [hep-ph]].
- [67] Z. Bern, G. Diana, L. J. Dixon, F. Febres Cordero, S. Hoeche, H. Ita, D. A. Kosower, D. Maitre, K.J. Ozeren, [arXiv:1106.1423 [hep-ph]].
- [68] W. Siegel, Phys. Lett. **B84**, 193 (1979); D. M. Capper, D. R. T. Jones, P. van Nieuwenhuizen, Nucl. Phys. **B167**, 479 (1980); L. V. Avdeev, A. A. Vladimirov, Nucl. Phys. **B219**, 262 (1983).
- [69] Z. Bern, D. A. Kosower, Nucl. Phys. **B379**, 451-561 (1992).
- [70] G. 't Hooft, M. J. G. Veltman, Nucl. Phys. **B44**, 189-213 (1972).